(REVISED)

C.P. No. 1340

PROCUREMENT EXECUTIVE, MINISTRY OF DEFENCE

AERONAUTICAL RESEARCH COUNCIL

CURRENT PAPERS

Evaluation of a Loading Form for the Calculation of Linearised Theory Pressure Distributions on Wings with Control Surfaces having Swept Hinge Lines in Steady Subsonic Flow

- by -

T.G. Wigley,

British Aircraft Corporation,

Military Aircraft Division, Warton

LONDON: HER MAJESTY'S STATIONERY OFFICE

1976

Price £2.60 Net

AERONAUTICAL RESEARCH COUNCIL

Mathematical Approaches to the Dynamics of Deformable Aircraft

Part I by A. S. Taylor

Part II by D. L. Woodcock

Reports and Memoranda No. 3776

CORRECTIONS

Page 15 Equation (P6). Delete "ρ" and insert "σ".

Page 26 Line 5. Delete "$m(r_{Rg} \times \dot{V})$" and insert "$m[(r_{Rg} \times \dot{V})$".

Page 45. Equations (116) last equation. Delete "$(\gamma+3)$" and insert "$(j+3)$".

Page 46. Line 14. Amend "euqations" to read "equations".

Line 17. Delete "w_j" and insert "ω_j".

Page 49. Line 4. Delete "X_i'" and insert "$\mathscr{X}_i'$".

Page 53. Line 8. Delete "X_∞" and insert "$X_{z\infty}$". Delete "$X_{z\infty}$" and insert "X_∞".

Page 81. Line 3. Amend "Lagrangeian" to read "Lagrangian".

Page 83. Line 1. Delete "$X_x x_1$" and insert "$Z_x x_1$".

Page 86. Line 2 (equation 20). Amend "
$$\begin{matrix} 0 & -r & q & \dot{x} \\ r & 0 & -p & \dot{y} \\ -q & p & 0 & \dot{z} \end{matrix}$$
to read
$$\begin{bmatrix} 0 & -r & q \\ r & 0 & -p \\ -q & p & 0 \end{bmatrix} \begin{bmatrix} \dot{x} \\ \dot{y} \\ \dot{z} \end{bmatrix}$$

Page 91. Third last line. Amend "$+\dot{v}_f$" to read "$\dot{v}_f$".

Page 92. Line 3. Amend "$I_z p_f r_f$" to read "$I_z) p_f r_f$".

Page 98. Line before equation (96). Delete "(84), (87), (90) and (93)" and insert "(85), (88), (91) and (94)".

Line before equation (97). Delete "(85), (88), (91), (92) and (94)" and insert "(86), (89), (92), (93) and (95)".

Page 103. Line 9 (below "Superscripts"). Insert "$'$".

Page 110. Line 9. Amend "presentative" to read "representative".

Page 113. Equation (C-23). Move "=" to the left to lie between the two matrices.

LONDON HER MAJESTY'S STATIONERY OFFICE
JUNE 1976

C.P. No.1340*
January 1975

EVALUATION OF A LOADING FORM FOR THE CALCULATION OF LINEARISED THEORY PRESSURE DISTRIBUTIONS IN WINGS WITH CONTROL SURFACES HAVING SWEPT HINGE LINES IN STEADY SUBSONIC FLOW

- by -
T.G. Wigley,
British Aircraft Corporation,
Military Aircraft Division, Warton

SUMMARY

Following suggestions made in BAC Preston Div. Rep. Ae 311 (BR 24598) 'partially matched' loadings are constructed to enable the accurate simulation of first order boundary conditions on wings with control surfaces having swept hinge lines in subsonic flow. These loadings are assessed by observing the character of the difference between the induced downwash and the required boundary condition, paying special attention to the neighbourhoods of hinge line corners. Finally, the 'regularised' downwashes are used in lifting surface calculations to provide values for the 'fully matched' loadings.

---

*Replaces A.R.C.35 865

Contents

Contents (Contd.)

1. INTRODUCTION

In Reference 1 a method is presented for determining first-order loading solutions on wings with control surfaces in steady subsonic flow. This method uses a 'partially matched' loading form, see section 2, which approximately satisfies the first order boundary condition and accounts for the main irregularities in downwash near control surface edges. The difference between the downwash field induced by the 'partially matched' loading and the required boundary condition is called the 'regularised' downwash.

Reference 1 contains satisfactory 'regularised' downwash distributions for rectangular wings having control surfaces with unswept hinge lines. However, results for a swept wing with a control surface configuration show residual singular downwash variations near the corners of the swept control surface.

An attempt was made, using special loading terms derived in Reference 2, to infer how the 'partially matched' loading form may be modified in order to adequately account for hinge line sweep effects. This document carries through the inference and presents the results of detailed calculations.

This work was carried out for the Ministry of Aviation Supply under research contract number K43A/421/CB4 3A2.

2. PROBLEM FORMULATION

In the jargon of Reference 2 it is useful to speak about 'inner' and 'outer' loading solutions. For example an 'inner' loading solution may be one valid in the close neighbourhood of a control surface corner, whereas a corresponding 'outer' solution may be that valid near the edge of the overall wing planform. The total 'inner' solution may be constrained to match the singular behaviour of the 'outer' solution in order to give a so-called 'partially matched' solution for a wing with a control surface configuration. Thus if it is desired to modify a given 'partially matched' loading form by incorporating a special 'inner' solution, care must be taken to ensure that the final form is still of a 'partially matched' type.

2.1 The Starboard Wing Inboard Corner Loading Solution

2.1.1 The 'inner' loading solution

In section 3.1.2 of Reference 2 a general solution is given for the starboard inboard corner loading which contains an infinite series of terms that account for swept hinge line effects. The dominant effect, found to be associated with the odd terms of the infinite series, was evaluated in Appendix J of Reference 1 and it is inferred in section 5 of Reference 1 that for a starboard wing control surface it might be beneficial to modify the 'partially matched' loading by incorporating the following sweep dependent singular 'inner' loading solution

$$\tfrac{1}{2}\bar{\Delta}C^{*}_{p_e} = \frac{\theta}{\pi\bar{\beta}} \cdot \frac{\zeta}{\bar{R}_e} \cdot \log\left[\frac{\bar{\beta}+m}{\bar{\beta}-m}\right] \qquad (1)$$

where $$\bar{R}_e = \sqrt{\zeta^2 + \bar{\beta}_e^2\,(\eta-\eta_e)^2} \qquad (2)$$

The procedure adopted in determining a closed form for the dominant sweep correction effect can be applied to find an expression for the residual dominant effect. This is found to be associated with the even terms in the above mentioned infinite series, and can also be incorporated into the 'inner' loading solution. This further loading modification takes the form

$$\tfrac{1}{2}\bar{\bar{\Delta}}C^{*}_{p_e} = -\frac{2\theta}{\pi\bar{\beta}} \cdot \frac{\bar{\beta}\,(\eta-\eta_e)}{\sqrt{(\zeta-\zeta_h)^2 + \bar{\beta}^2\,(\eta-\eta_e)^2}} \cdot \frac{1}{2}\log\left[1 - \left(\frac{m}{\bar{\beta}}\right)^2\right] \qquad (3)$$

The analytic integration of equation (1) to give local singular downwash variations is carried out in section 5 of Reference 1. A similar treatment of equation (3) leads to the following expression for local downwash

$$\delta w_{2f} = \frac{\theta}{4\pi^2} \cdot \frac{\bar{\beta}\,\bar{\bar{\eta}}_s\,\mathrm{sgn}\,(\zeta_r)}{\sqrt{\bar{c}_1^2\,\zeta_r^2 + \bar{\beta}^2\,\bar{\bar{\eta}}_s^2}} \cdot \log\left[1 - \left(\frac{m}{\bar{\beta}}\right)^2\right] \cdot$$

$$\left\{\log\left[\bar{\beta}\,\bar{\bar{\eta}}_s\right]^2 - 2\log\left[\sqrt{\bar{c}_1^2\,\zeta_r^2 + \bar{\beta}^2\,\bar{\bar{\eta}}_s^2} + \bar{c}_1|\zeta_r|\right]\right\} \qquad (4)$$

where $$\bar{\bar{\eta}}_s = \eta_s - \eta_e$$

In equation (4) when

1) $\zeta_r = 0.$, $\delta w_{2f} = 0.$

and $|\zeta_r| > 0.$, δw_{2f} is antisymmetric about $|\eta_s-\eta_e| = 0.$

2) $|\eta_s-\eta_e| = 0.$, $\delta w_{2f} = 0.$

and $|\eta_s-\eta_e| > 0.$, δw_{2f} is antisymmetric about $\zeta_r = 0.$

Results of calculations using equation (4) are presented and discussed in section 4.2.

2.1.2 The formation of a 'partially matched' loading modification

The additive 'inner' loading modification must be matched to 'outer' solution singular behaviours in a manner consistent

with the original 'partially matched' loading form. To achieve the matching, loading factors $C(\zeta,\eta)$, $F(\eta)$ are applied to the 'inner' loading modification where at the leading or trailing edge boundaries

$$\left.\begin{aligned} C(\zeta,\eta) &= \sqrt{1-\zeta}\cdot\sqrt{1+\frac{\zeta}{\zeta_1}}\cdot\left\{1-\frac{\zeta}{2}\left[\frac{1}{\zeta_1}-1\right]\right\} \\ \zeta_1 &= \frac{\left[x_h(\eta)-x_1(\eta)\right]}{c_1(\eta)} = \frac{c_2(\eta)}{c_1(\eta)} \end{aligned}\right\} \qquad (5)$$

and at the inboard side edges and wing tips of the control surfaces

$$\begin{aligned} F(\eta) &= F_1(\eta) \quad \text{for} \quad \eta \geq \eta_e \\ &= F_2(\eta) \quad \text{for} \quad \eta < \eta_e \end{aligned}$$

The functions $F_1(\eta)$, $F_2(\eta)$ have the following properties

$$\begin{aligned} F_1(\eta) &\sim \sqrt{1-\eta} \quad \text{as} \quad \eta \to 1 \\ F_1(\eta) &\to 1 \quad \text{as} \quad (\eta-\eta_e) \to 0_+ \end{aligned}$$

where η_e is the spanwise location of the inboard edge of the starboard control surface.

$$\begin{aligned} F_2(\eta) &\sim \sqrt{1+\eta} \quad \text{as} \quad \eta \to -1 \\ F_2(\eta) &\to 1 \quad \text{as} \quad (\eta-\eta_e) \to 0_- \end{aligned}$$

and they are continuous up to and including third derivative at $\eta = \eta_e$. The functions are

$$\left.\begin{aligned} F_1(\eta) &= \sqrt{\frac{1-\eta}{1-\eta_e}}\cdot\left[1+\frac{1}{2}\left(\frac{\eta-\eta_e}{1-\eta_e}\right)+\frac{3}{8}\left(\frac{\eta-\eta_e}{1-\eta_e}\right)^2+\frac{5}{16}\left(\frac{\eta-\eta_e}{1-\eta_e}\right)^3\right] \\ F_2(\eta) &= \sqrt{\frac{1+\eta}{1+\eta_e}}\cdot\left[1-\frac{1}{2}\left(\frac{\eta-\eta_e}{1+\eta_e}\right)+\frac{3}{8}\left(\frac{\eta-\eta_e}{1+\eta_e}\right)^2-\frac{5}{16}\left(\frac{\eta-\eta_e}{1+\eta_e}\right)^3\right] \end{aligned}\right\} \qquad (6)$$

The 'partially matched' loading modification associated with the port inboard hinge line corner is calculated by setting η to $-\eta$ in equations 1 to 6.

2.2 The Starboard Wing Tip Corner Loading Solution

2.2.1 The 'inner' loading solution

The 'inner' tip corner loading solution, derived in Reference 6, is expressed as

$$\tfrac{1}{2}\Delta C^{*}_{p_t} = -\frac{\theta}{\pi\bar{\beta}} \cdot \frac{m}{\bar{\beta}} \left[1 + \frac{1}{32}\left(\frac{m}{\bar{\beta}}\right)^2\right] \cdot \sqrt{2\bar{\beta}_t(1-\eta)} \cdot \frac{\zeta}{\bar{R}_t \sqrt{\bar{R}_t + \bar{\beta}_t(1-\eta)}} \tag{7}$$

where $\bar{R}_t$ is given by

$$\bar{R}_t = \sqrt{\zeta^2 + \bar{\beta}_t^2(1-\eta)^2} \tag{8}$$

2.2.2 The formation of a 'partially matched' loading modification

Equation (7) already has the correct starboard tip behaviour, therefore, in a spanwise sense, it is only necessary to apply a port tip factor defined by

$$H = \sqrt{1+\eta} \cdot [-A\eta^3 + B\eta^2 - C\eta + D] \tag{9}$$

for $-1 \leq \eta \leq -\eta_2$

and $H = 1$ (10)

for $\eta \geq -\eta_2$ where H is continuous up to and including third derivative at $\eta = -\eta_2$ and A, B, C and D are coefficients defined in Appendix C of Reference 1.

The 'partially matched' loading modification associated with the port tip hinge line corners is calculated by setting η to $-\eta$ in equations (7) to (9).

The wing leading and trailing edge singularities are again accounted for by the factor $C(\zeta,\eta)$ given in equation (5).

3. THE FORMS OF MODIFIED LOADING AND THEIR USE

3.1 The Definition of 'Regularised' Downwash

In Reference 5 an integral equation is presented which relates the normal velocity, or downwash, to the pressure difference, or loading, in subsonic flow and takes the form

$$w(x_r,y_s) = -\frac{1}{8\pi}\int\int_S \Delta C_p . K(X,Y;M)\, dy\, dx \qquad (11)$$

where $K(X,Y;M)$ is the Kernel function.

Now ΔC_p can be expressed by

$$\Delta C_p = {}_2\Delta C_p^* - {}_1\Delta C_p \qquad (12)$$

where ${}_2\Delta C_p^*$ contains the irregular loading effects ${}_2\Delta C_p$, defined in Reference 1, together with extra 'partially matched' loading modifications ${}_2\bar{\Delta}C_{p_e}^*$ and ${}_2\bar{\Delta}C_{p_t}^*$. ${}_1\Delta C_p$ is a loading of the type associated with smoothly distorted wings.

The relationship between downwash and total pressure coefficient in equation (11) allows a definition for downwash corresponding to equation (12) to be written

$$w = w_2^* - w_1 \qquad (13)$$

where $w = 0.$ for points off the control surface

$= \theta$ for points on the control surface, where θ is the control surface deflection in radians

and w_2^* is the irregular downwash corresponding to ${}_2\Delta C_p^*$.

A 'regular' downwash w_1 is thus defined by

$$w_1 = w_2^* - w \ . \qquad (14)$$

It follows from this definition that if the dominant irregular loading effects are properly accounted for then w_1 will take the form of a downwash field suitable for use in an ordinary lifting surface calculation. This, in turn, provides values of ${}_1\Delta C_p$ which, through equation (12), give the 'fully matched' solution ΔC_p.

3.2 <u>The Implementation of the 'Partially Matched' Loading Modification in the Spanwise Integrations Including Contributions to the Coefficients of the Log Singularity Terms</u>

The formation of the final 'partially matched' loading involves addition of the 'partially matched' loading modification to the loading form previously defined in Reference 1. The final starboard wing 'partially matched' loading modification is

$$T_s = {}_2\bar{\Delta}C_p^* = \frac{\theta}{\pi\bar{\beta}}\left\{F(\eta)\cdot\frac{\zeta}{\bar{R}_e}\cdot\frac{1}{2}\log\left[\frac{\bar{\beta}+m}{\bar{\beta}-m}\right]\right.$$
$$\left. -H(\eta)\cdot\frac{m}{\bar{\beta}}\left[1+\frac{1}{32}\left(\frac{m}{\bar{\beta}}\right)^2\right]\frac{\zeta}{\bar{R}_t}\cdot\sqrt{\frac{2\bar{\beta}_t(1-\eta)}{\bar{R}_t+\bar{\beta}_t(1-\eta)}}\right\} C(\zeta,\eta) \qquad (15)$$

where $C(\zeta,\eta)$, $F(\eta)$ are as defined in section 2.1.2

T_s, along with the corresponding port term, T_p, are required in the evaluation of the coefficients of the log singularity terms.

The chordwise integration of $\log \bar{\zeta}$, $\bar{\zeta} \log \bar{\zeta}$ type singularities contained in the spanwise integral $L(\zeta)$ discussed in Reference 1 require special treatment as $|\zeta-\zeta_r| \to 0$. The special numerical treatment also requires that the value, together with the first and second derivatives of the 'partially matched' loading be evaluated to form the coefficients of the log singularity terms. It follows then that a similar treatment must now be adopted in treating the modified partially matched loading. Expressions used in determining the coefficients of these singularities (a_{p_i}, a_{q_i}) derived from the starboard wing 'partially matched' loading appear in Appendix A.

The modified singular loading expression at (ζ_r, η_s) for a tapered wing planform with control surfaces having smooth swept hinge lines is

$$l_2^*(\zeta_r,\eta_s) = l_2(\zeta_r,\eta_s) + T_s + T_p \qquad (16)$$

where from Appendix B of Reference 1

$$\left.\begin{aligned} l_2(\zeta_r,\eta_s) &= g_1(L_1+L_2+L_3+L_4) + g_2(L_5+L_6+L_7+L_8) \quad , \quad \eta_s < \eta_e \\ &= g_1(\bar{L}_1+L_2+L_3+L_4) + g_2(L_5+L_6+L_7+L_8) \\ &\quad + g_1 \log \zeta^2 \quad , \quad \eta_s > \eta_e \end{aligned}\right\} \qquad (17)$$

is the final unmodified 'partially matched' loading. Also,

T_s is the final starboard 'partially matched' loading modification, see equation (15), and

T_p is the final port 'partially matched' loading modification.

g_1, g_2 contain loading factors and sweep and taper dependent terms.

Equation (16) and the expressions in Appendix A are used in determining the coefficients of the log singularities in a similar manner to that described in Appendix B of Reference 1.

4. CALCULATION METHOD AND DISCUSSION OF THE RESULTS

The numerical methods discussed in this document have been programed in Fortran IV for an IBM 360/65 computer and the results presented in the following sections.

4.1 Introduction to the Discussion of Results

To demonstrate the effectiveness of the 'partially matched' loading modification in removing residual irregular downwash variations near

the corners of swept control surfaces, results for the 'regularised' downwash field due to the modified loading are compared in section 4.2 with those for the loading of Reference 1 at M = 0.0, 0.8 for the planform shown in Figure 1A. This untapered wing is of aspect ratio 4 and, outboard of $|\eta| = 0.2$, is swept back at an angle $\Lambda = 45°$ whilst, inboard of $|\eta| = 0.2$, the planform is smoothly rounded in the manner detailed in Reference 4. The control surfaces are located in $0.5 < |\eta| < 1.0$ having smooth constant percentage chord hinge lines along $\zeta = 0$.

The downwash fields presented in section 4.2 are modified in the neighbourhood of the inboard corner by using equation (4) of section 2.1.1.

In subsection 4.3.1, three orders of Multhopp collocation point distributions have been selected to compare 'regularised' downwash fields produced with and without loading modification. In subsection 4.3.2 the 'regularised' downwash field defined at collocation points for (m,n) = (16,6) is used in lifting surface calculations to produce 'interpolated' downwash values and in 4.3.3 to calculate 'fully matched' loadings.

In 4.4.2 total pressure distributions and generalised forces results at M = 0.8 are presented for the Royal Aircraft Establishment's Wing A (shown in Figure 1B) with control surfaces located in $0.4 < |\eta| < 0.7$ having smooth hinge lines on $\zeta = 0$.

4.2 Preliminary Calculations with the 'Partially Matched' Modified Loading Form

In Reference 1, Figure 16, spanwise downwash distributions are presented for the swept wing planform shown in Figure 1A using a simple form of 'partially matched' loading. The spanwise downwash distributions at $\zeta = \pm 0.03$ either side of the swept hinge line $\zeta = 0.0$ are characterised by peaks in the neighbourhoods of the starboard wing hinge line control surface corners. To demonstrate the effectiveness of the modified 'partially matched' loading solution in removing the most significant irregular downwash variations comparisons of spanwise downwash distributions at $\zeta = \pm 0.03$ for M = 0.0, 0.8 are presented in Figures 2 and 3 produced using modified and unmodified loading definitions.

In Reference 1 special consideration is given to integrations involving $|\eta_e - \eta|$ and ζ small, that is, when a solution point (ζ,η) is placed very close to the hinge line corners. It is found that an inordinate effort is required to maintain calculation accuracy in these regions and for this reason the downwash curves are not continuous across η_e. The restrictions on the positioning of a solution point (ζ,η) are defined at a swept hinge line corner by

$$|\zeta| > 0.03 \quad \text{and} \quad |\eta - \eta_e| > 0.01$$

and at a swept hinge line tip by

$$|\zeta| > 0.03 \quad \text{and} \quad |\eta| < 0.99$$

Figure 2A presents spanwise downwash distributions at $\zeta = -0.03$ with M = 0.0 for the loading of Reference 1, the first modified form and second modified form. Discussions concerning results for the second modified form are given later in this section. As is clearly demonstrated in Figure 2A singularities in the neighbourhoods of the starboard hinge line corners have been removed to produce a 'regularised' downwash distribution. There is still a residual effect present in the immediate neighbourhood of the inboard starboard hinge line corner but it is of a much lower order. In Figure 2B, for $\zeta = 0.03$, similar comments hold. The comments applied above to Figures 2A, 2B can also be applied to 3A, 3B although in the latter two figures the irregularities are exagerated by the presence of a Mach number related effect in the loading forms.

Expression (4) of section 2.1.1 has been used to provide modifications to the local downwash in the neighbourhood of the inboard swept hinge line corner for the planform of Figure 1A. The results are presented on Figures 2 and 3 and are denoted by dashed lines. As can be seen in Figures 2A, 2B a more 'regular' downwash is produced in the neighbourhood of the starboard inboard corner. In Figures 3A, 3B for M = 0.8 the effect of using the second modified form is to again produce a more 'regularised' downwash distribution.

4.3 Schemes for Evaluating the Effectiveness of the Modified Loading Form

The preliminary calculations discussed in section 4.2 have demonstrated that the proposed 'partially matched' loading modification does give rise to 'regular' downwash variations in the neighbourhoods of control surface corners. The final step in this evaluation is to calculate 'fully matched' loadings produced by lifting surface calculations using the 'partially matched' loading modification.

4.3.1 'Regularised' downwash fields for three Multhopp collocation point distributions

Three orders of Multhopp collocation point distributions have been chosen for comparative purposes: (m,n) = (12,6), (12,8) and (16,6) for which 'regularised' downwash distributions have been produced using the 'partially matched' unmodified loading (Figures 4A to 9A) and the first modified loading (Figures 4B to 9B).

A similar comparative exercise to that carried out in section 4.1 close to the hinge line can now be repeated for the more general spacing of solution points specified by the three Multhopp collocation point distributions. The comparison involves considering relative 'regularity' in downwash in the neighbourhoods of the corners of the starboard control surface of the corresponding A and B Figures. It is evident from comparing corresponding A and B Figures that more 'regular' downwash distributions are presented in the B Figures than the A. Of the spanwise plots Figures 6A, 6B and of the chordwise plots Figures 9A, 9B best illustrate the 'regularising' effect produced by use of the modified

'partially matched' loading. The comparisons made are confined to considering relative 'regularity' in downwash because the downwash fields presented have been obtained using different loading forms. The comments made above refer to 'regularised' downwash fields calculated at Multhopp collocation points which can be used in conjunction with the lifting surface scheme of Reference 4 to provide the loading ($_1\Delta C_p$) defined in equation (12). This 'regularised' loading can then be combined with the irregular loading to provide a fully matched loading. A method for measuring the accuracy with which the lifting surface calculation scheme fits 'regularised' downwash distributions is discussed in section 4.3.2.

4.3.2 Interpolation of 'regularised' downwash fields

A simplified matrix form of the equation solved in Reference 4 is

$$w = b\,A \qquad (18)$$

where w is the regularised downwash matrix
b is the loading matrix
and A is the influence coefficient matrix

Downwashes given at a set of collocation points can be used to generate a loading matrix which, in conjunction with a recalculated influence coefficient matrix, can be used to calculate 'interpolated' downwash values at any specified set of points. The difference, E, between the 'regularised' downwashes, calculated in the manner described in this document, and the 'interpolated' downwashes calculated at corresponding points, gives a measure of how accurately the 'regularised' downwash field is fitted by the lifting surface calculation scheme.

With the Multhopp collocation distribution (m,n) = (16,6) at M = 0.0 for the test case planform of Figure 1A, spanwise error distributions are presented in Figures 10 to 12 for three chordwise stations at $\bar{x}$ = 0.677302, 0.874255 and 0.985471, the hinge line being at $\bar{x}$ = 0.75. Chordwise error distributions are presented in Figures 13 to 15 for the three spanwise stations η = 0.445738, 0.602635 and 0.982973, the control surface edge being at η = 0.5. Comparing the error distributions obtained from the modified and unmodified 'partially matched' loadings, from Figures 10 to 15, the magnitude of the error distribution obtained using the modified loading form is less than that obtained with the unmodified loading form. This is most significant close to the inboard corner and hinge line tip corner (see Figures 10 and 15). Where the magnitude of the error distribution obtained using the modified loading form is not less than that for the unmodified loading the overall error magnitude is relatively small.

4.3.3 'Fully matched' loading distributions

Using the 'regularised' downwash field presented in section 4.3.1 for the Multhopp collocation point distribution, (m,n) = (16,6), 'regularised' loadings have been calculated for the modified 'partially matched' loading presented in this document. The 'regularised' loadings ($_1\Delta C_p$) have been calculated using the lifting surface scheme described in Reference 4 and combined with the corresponding irregular loadings ($_2\Delta C_p$) to form 'fully matched' loading distributions (ΔC_p).

The 'fully matched' loading distributions at M = 0.0 for the test case planform of Figure 1A are presented in Figures 16 and 17. In Figure 16 chordwise ΔC_p distributions are presented at η stations η = 0.0, 0.3, 0.4, 0.45, 0.475, 0.5 the control surface edge being at η = 0.5 and the hinge line at $\bar{x}$ = 0.75. In Figure 17 chordwise ΔC_p distributions are presented for η = 0.5, 0.525, 0.7, 0.95, 0.98. ΔC_p along η = 0.5 is repeated for comparative purposes.

4.4 Presentation of the Results Obtained Using the R.A.E. Wing A with Control Surfaces for M = 0.8

The Wing A planform, shown in Figure 1B, has been smoothly rounded inboard of $|\eta|$ = 0.19509, after the manner described in Reference 4, as required by the numerical scheme used. Control surfaces are located in $0.4 < |\eta| < 0.7$.

4.4.1 The definition of integrated quantities

The control surface deflection δ in radians is measured in a streamwise plane normal to the planform, the fully matched pressure is ΔC_p and the force mode is Z_i. The generalised force definition for unit deflection is

$$Q_i = \int_{-1}^{1} \int_{x_1(\eta)}^{x_t(\eta)} Z_i \, \Delta C_p \, dx \, d\eta \qquad (19)$$

For the control surface angle measured about the hinge line ΔC_p becomes $\Delta C_p/\delta \cos \Lambda_h$ and Z_i becomes $Z_i \cos \Lambda_h$ where Λ_h is the hinge line sweep angle.

For unit angle of deflection, δ, the lift is

$$L = \int_{-1}^{1} \int_{x_1(\eta)}^{x_t(\eta)} \Delta C_p \, dx \, d\eta \qquad (20)$$

the pitching moment about an axis through the wing apex is

$$M = \int_{-1}^{1} \int_{x_1(\eta)}^{x_t(\eta)} [x(\eta)-x_1(\eta)]\ \Delta C_p\ dx\ d\eta \tag{21}$$

the hinge moment is

$$H = \int_{-1}^{1} \int_{x_1(\eta)}^{x_t(\eta)} [x_h(\eta)-x(\eta)]\ \Delta C_p\ dx\ d\eta \tag{22}$$

the rolling moment on the half wing about the centre line $\eta = 0$ is

$$B = \int_{0}^{1} \int_{x_1(\eta)}^{x_t(\eta)} \eta\ \Delta C_p\ dx\ d\eta \tag{23}$$

the non-dimensionalised spanwise loading is

$$\frac{c(\eta)\ C_{LL}}{\bar{c}(\eta)\ C_L} = \frac{2s}{L} \int_{x_1(\eta)}^{x_t(\eta)} \Delta C_p\ dx \tag{24}$$

where
- $c(\eta)$ is the local chord of the wing
- $\bar{c}(\eta)$ is the mean chord $S/2s$
- C_{LL} is the lift per unit span$/(\frac{1}{2}\ \rho\ U^2\ c)$
- $c_\delta(\eta)$ is the local chord of the control surface
- C_L is $L/(\frac{1}{2}\ \rho\ U^2\ S)$
- S is the planform area of the wing
- s is the semi-span of the wing

the local centre of pressure is

$$X_{cp} = \frac{1}{c(\eta)} \frac{\int_{x_1(\eta)}^{x_t(\eta)} \Delta C_p\ [x(\eta)-x_1(\eta)]\ dx}{\int_{x_1(\eta)}^{x_t(\eta)} \Delta C_p\ dx} \tag{25}$$

where x_h is the local ordinate of the hinge line,

and the non-dimensionalised spanwise hinge moment is

$$\frac{c_\delta^2 C_{HL}}{\bar{c}_\delta^2 C_H} = \frac{s_\delta}{H} \int_{x_1(\eta)}^{x_h(\eta)} [x_h(\eta)-x(\eta)]\, \Delta C_p \, dx \qquad (26)$$

where
- C_{HL} is the hinge moment per unit span/$(\frac{1}{2} \rho U^2 c_\delta^2)$
- C_H $H/(\frac{1}{2} \rho U^2 S_\delta \bar{c}_\delta)$
- s_δ is the span of the control surface $[s(\eta_o-\eta_i)]$
- η_i, η_o are the inboard and outboard edge of the control surface
- $\bar{c}_\delta$ representative length of control $[S_\delta/s_\delta]$

4.4.2 Discussion of the results

The results presented in Tables 1 to 4 and Figures 18 to 24 have been obtained from 'regularised' downwashes for a Multhopp collocation distribution of order (m,n) = (12,9). The 'fully matched' loading $\Delta C_p/\delta \cos \Lambda_h$ and integrated effects have been calculated for the $(\bar{x},\eta)$ distributions shown in Tables 1 to 4 and presented graphically in Figures 18 to 24.

5. CONCLUSIONS

Use was made of the special loading terms derived in Reference 2 to infer how the 'partially matched' loading form of Reference 1 should be modified to adequately account for hinge line sweep effects. The modified 'partially matched' loading form described in this document has been used to produce downwash fields on planforms with swept hinge lines without the appearance of the irregularities in downwash discussed in Reference 1.

By checking the accuracy with which 'regularised' downwash distributions can be represented by a lifting surface calculation procedure, it has been successfully demonstrated that the current form of modified loading should lead to accurate 'fully matched' solutions.

Pressure difference distributions, locally integrated effects and generalised forces have been calculated and presented for the R.A.E. Wing A geometry, modified in the centre section region as shown in Figure 1B, with control surfaces located in $0.4 < |\eta| < 0.7$ for M = 0.8.

6. A GLOSSARY OF MAIN SYMBOLS

- A Aspect ratio of a wing planform
- c Local chord of wing
- c_i Local chord of control surface

$\bar{c}_1$	c_1/s
c_2	$c - c_1$
$C(\zeta,\eta)$	Loading factor in the chordwise sense (see equation (5))
E	Error function (see section 4.3.2)
$F(\eta)$	Loading factor in the spanwise sense (see section 2.1.2)
$H(\eta)$	Loading factor in the spanwise sense (see section 2.2.2)
$K(X,Y;M)$	Kernel function (see equation (11))
$L(\zeta)$	The spanwise integral
$l_2^*(\zeta_r,\eta_s)$	See equation (16)
M	Mach number
m	$\left(\frac{dx_h}{d\eta}\right)_{\eta_e}$
$\bar{R}_e$	See equation (2)
$\bar{R}_t$	See equation (8)
s	Semispan
T_s	Final spanwise 'partially matched' loading modification (see equation (15))
$w(x_r,y_s)$	Downwash distribution
$w_1(x_r,y_s)$	See section 3.1
$w_2(x_r,y_s)$	See section 3.1
$w_2^*(x_r,y_s)$	See section 3.1
x	Cartesian coordinate in free stream direction
$\bar{x}$	$(x-x_l)/c$
$x_h(\eta)$	Equation of the hinge line of the control surface
$x_l(\eta)$	Equation of the leading edge of the wing
x_r	Streamwise coordinate of collocation station
$x_t(\eta)$	Equation of the trailing edge of the wing
y	Cartesian coordinate in the spanwise direction
y_s	Spanwise coordinate of collocation station

β	$\sqrt{1-M^2}$
$\bar{\beta}$	$\sqrt{\beta^2+m^2}$
$\bar{\beta}_e$	$\bar{\beta}/\bar{c}_1(\eta_e)$
$\bar{\beta}_t$	$\bar{\beta}/\bar{c}_1(1)$
δw_{2f}	See equation (4)
$\Delta C_p(x,y)$	See section 3.1
${}_1\Delta C_p(x,y)$	See section 3.1
${}_2\Delta C_p(x,y)$	See section 3.1
${}_2\bar{\Delta}C^*_{pe}$	${}^1_2\bar{\Delta}C^*_{pe} + {}^2_2\bar{\Delta}C^*_{pe}$
${}_2\bar{\Delta}C^*_{pt}$	${}^1_2\bar{\Delta}C^*_{pt} + {}^2_2\bar{\Delta}C^*_{pt}$
${}_2\Delta C^*_p(x,y)$	See section 3.1
${}^1_2\bar{\Delta}C^*_{pe}$	See equation (1)
${}^1_2\bar{\bar{\Delta}}C^*_{pe}$	See equation (3)
${}^1_2\bar{\Delta}C^*_{pt}$	See equation (7)
ζ	Non-dimensional coordinate $\frac{x(\eta)-x_h(\eta)}{c_1(\eta)}$
ζ_r	ζ coordinate of collocation station
$\bar{\zeta}$	$\zeta-\zeta_r$
ζ_h	ζ coordinate of the hinge line
ζ_1	See equation (5)
η	y/s
η_e	Coordinate of side edge of control surface
η_s	Spanwise coordinate of collocation station
$\bar{\bar{\eta}}_s$	$\eta_s-\eta_e$
η_1	Outboard limit of centre section rounding region
η_2	See section 2.2.2
θ	Control surface deflection
Λ	Sweep angle on a wing planform

7. REFERENCES

1. Marchbank, W. R.
   Kennelly, J. M.
   Hewitt, B. L.

   The evaluation of pressure distributions on wings with control surfaces in subsonic flow.

   B.A.C. Preston Divn. Report Ae 311, November, 1970

2. Hewitt, B. L.

   Unsteady airforces for wings with control surfaces.

   Paper No. 14, Part I, AGARD Symposium on Unsteady Aerodynamics for Aeroelastic Analyses of Interfering Surfaces.

   Tønsberg, Oslofjorden, Norway
   November, 3-4, 1970

3. Hewitt, B. L.
   Kellaway, W. E. R.

   A new treatment of the subsonic lifting surface problem using curvilinear coordinates.

   Part I Details of the method as applied to regular surfaces with finite tip chords and a preliminary set of numerical results.

   B.A.C. Preston Divn. Report Ae 290, August, 1968

4. Kellaway, W.

   A new treatment of the subsonic lifting surface problem using curvilinear coordinates.

   Part III Details of computer programs

   B.A.C. Preston Divn. Report Ae 290, May, 1969

5. Hewitt, B. L.
   Wallace, B. A.

   On the derivation and application of linearised theory expressions for the induced velocity field around an oscillating lifting surface.

   B.A.C. Preston Divn. Report Ae 246, September, 1965

6. Hewitt, B. L.
   Marchbank, W. R.

   Special loading functions for treating wings with control surfaces in unsteady, subsonic flow.

   B.A.C. (M.A.D.) Report Ae 345, (To be published)

APPENDIX A

The 'Partially Matched' Loading Modification, First and Second Derivative as Required in the Calculation of the Coefficients of the Log Singularity Terms

In the expression for the final starboard 'partially matched' wing loading modification, T_s, see equation (15) of section 3.2, let

$$q_1 = \frac{\theta}{\pi\bar{\beta}} \cdot \zeta \cdot \frac{1}{2} \log \left[\frac{\bar{\beta}+m}{\bar{\beta}-m}\right]$$

$$q_2 = -\frac{\theta}{\pi\bar{\beta}} \cdot \frac{m}{\bar{\beta}} \left[1 + \frac{1}{32}\left(\frac{m}{\bar{\beta}}\right)^2\right] \cdot \zeta$$

then
$$T_s = \left\{ q_1 \frac{F(\eta)}{\bar{R}_e} + H(\eta) \cdot \frac{q_2}{\bar{R}_t} \cdot \sqrt{\frac{2\bar{\beta}_t(1-\eta)}{\bar{R}_t+\bar{\beta}_t(1-\eta)}} \right\} \cdot C(\zeta,\eta) \qquad (A1)$$

where $C(\zeta,\eta)$, $F(\eta)$ are defined in section 2.1.2

and $H(\eta)$ is defined in section 2.2.2

Let
$$T_1 = \frac{q_1 \cdot F(\eta)}{\bar{R}_e}, \qquad T_{s1} = T_1 \cdot C(\zeta,\eta) \qquad (A2)$$

Then
$$\frac{dT_{s1}}{d\eta} = \left[\frac{q_1}{\bar{R}_e} \cdot \frac{dF}{d\eta} - T_1 \cdot \frac{\bar{\beta}_e^2}{\bar{R}_e}(\eta-\eta_e)\right] \cdot C + \frac{q_1 \cdot F}{\bar{R}_e} \cdot \frac{dC}{d\eta} \qquad (A3)$$

and
$$\left.\begin{aligned} \frac{d^2T_{s1}}{d\eta^2} = {} & \left\{ \frac{q_1}{\bar{R}_e}\left[\frac{d^2F}{d\eta^2} - \frac{dF}{d\eta} \cdot \frac{\bar{\beta}_e^2(\eta-\eta_e)}{\bar{R}_e^2}\right] - \frac{dT_1}{d\eta} \cdot \bar{\beta}_e^2 \frac{(\eta-\eta_e)}{\bar{R}_e^2} \right. \\ & \left. + \frac{T_1 \cdot \bar{\beta}_e^2}{\bar{R}_e^2}\left[\frac{2\bar{\beta}_e^2(\eta-\eta_e)^2}{\bar{R}_e^2} - 1\right] \right\} \cdot C \\ & + 2 \cdot \left[\frac{q_1}{\bar{R}_e} \cdot \frac{dF}{d\eta} - \frac{T_1 \cdot \bar{\beta}_e^2(\eta-\eta_e)}{\bar{R}_e}\right] \cdot \frac{dC}{d\eta} + \frac{q_1 \cdot F}{\bar{R}_e} \cdot \frac{d^2C}{d\eta^2} \end{aligned}\right\} \qquad (A4)$$

Let
$$T_2 = \frac{q_2}{\bar{R}_t} \cdot \sqrt{\frac{2\bar{\beta}_t(1-\eta)}{\bar{R}_t+\bar{\beta}_t(1-\eta)}}\,, \quad T_{s_2} = T_2 . H(\eta) . C(\zeta,\eta) \tag{A5}$$

$$\left.\begin{aligned}\frac{dT_{s_2}}{d\eta} &= T_2 \cdot \left\{ \frac{\bar{\beta}_t^2(1-\eta)}{\bar{R}_t^2} + \frac{\bar{\beta}_t(1-\eta)-\bar{R}_t}{2\bar{R}_t(1-\eta)} \right\} \cdot H \cdot C \\ &\quad + \frac{q_2}{\bar{R}_t} \cdot \sqrt{\frac{2\bar{\beta}_t(1-\eta)}{\bar{R}_t+\bar{\beta}_t(1-\eta)}}\, \frac{d}{d\eta}(H \cdot C)\end{aligned}\right\} \tag{A6}$$

$$\left.\begin{aligned}\frac{d^2T_{s_2}}{d\eta^2} &= \left\{ \frac{dT_2}{d\eta}\left[\frac{\bar{\beta}_t^2(1-\eta)}{\bar{R}_t^2} + \frac{\bar{\beta}_t}{2\bar{R}_t} - \frac{1}{2(1-\eta)} \right] \right. \\ &\quad \left. + T_2 \left[\frac{\bar{\beta}_t^2[2\bar{\beta}_t^2(1-\eta)^2-\bar{R}_t^2]}{\bar{R}_t^4} + \frac{\bar{\beta}_t^3(1-\eta)}{2\bar{R}_t^3} - \frac{1}{2(1-\eta)^2} \right] \right\} .H.C \\ &\quad + 2.T_2 \left\{ \frac{\bar{\beta}_t^2(1-\eta)}{\bar{R}_t^2} + \frac{\bar{\beta}_t(1-\eta)-\bar{R}_t}{2\bar{R}_t(1-\eta)} \right\} \cdot \frac{d}{d\eta}(H.C) \\ &\quad + \frac{q_2}{\bar{R}_t} \cdot \sqrt{\frac{2\bar{\beta}_t(1-\eta)}{\bar{R}_t+\bar{\beta}_t(1-\eta)}} \cdot \frac{d^2}{d\eta^2}(H.C)\end{aligned}\right\} \tag{A7}$$

The functions T_{s_1}, T_{s_2} and their derivatives involve the functions $C(\zeta,\eta)$, $F(\eta)$, $H(\eta)$.

Let
$$\left.\begin{aligned}F_1(\eta) &= \sqrt{\frac{1-\eta}{1-\eta_e}} \cdot f_1(\eta) \\ f_1(\eta) &= \left[1 + \frac{1}{2}\left(\frac{\eta-\eta_e}{1-\eta_e}\right) + \frac{3}{8}\left(\frac{\eta-\eta_e}{1-\eta_e}\right)^2 + \frac{5}{16}\left(\frac{\eta-\eta_e}{1-\eta_e}\right)^3 \right]\end{aligned}\right\} \tag{A8}$$

then
$$\left.\begin{aligned}\frac{dF_1}{d\eta} &= \frac{-f_1}{2\sqrt{(1-\eta_e)(1-\eta)}} + \sqrt{\frac{1-\eta}{1-\eta_e}} \cdot \frac{df_1}{d\eta} \\ \frac{df_1}{d\eta} &= \frac{1}{2(1-\eta_e)}\left[1 + \frac{3}{2}\left(\frac{\eta-\eta_e}{1-\eta_e}\right) + \frac{15}{8}\left(\frac{\eta-\eta_e}{1-\eta_e}\right)^2 \right]\end{aligned}\right\} \tag{A9}$$

and

$$\frac{d^2F_1}{d\eta^2} = \frac{-f_1}{4\sqrt{1-\eta_e}\cdot(1-\eta)^{3/2}} - \frac{df_1/d\eta}{\sqrt{(1-\eta_e)(1-\eta)}} + \sqrt{\frac{1-\eta}{1-\eta_e}}\cdot\frac{d^2f_1}{d\eta^2}$$

$$\frac{d^2f_1}{d\eta^2} = \frac{3}{4(1-\eta_e)^2}\cdot\left[1+\frac{5}{2}\left(\frac{\eta-\eta_e}{1-\eta_e}\right)\right] \qquad (A10)$$

Let

$$F_2(\eta) = \sqrt{\frac{1+\eta}{1+\eta_e}}\cdot f_2(\eta)$$

$$f_2(\eta) = \left[1-\frac{1}{2}\left(\frac{\eta-\eta_e}{1+\eta_e}\right)+\frac{3}{8}\left(\frac{\eta-\eta_e}{1+\eta_e}\right)^2-\frac{5}{16}\left(\frac{\eta-\eta_e}{1+\eta_e}\right)^3\right] \qquad (A11)$$

then

$$\frac{dF_2}{d\eta} = \frac{f_2}{2\sqrt{(1+\eta_e)(1+\eta)}} + \sqrt{\frac{1+\eta}{1+\eta_e}}\cdot\frac{df_2}{d\eta}$$

$$\frac{df_2}{d\eta} = \frac{-1}{2(1+\eta_e)}\left[1+\frac{3}{2}\left(\frac{\eta-\eta_e}{1+\eta_e}\right)-\frac{15}{8}\left(\frac{\eta-\eta_e}{1+\eta_e}\right)^2\right] \qquad (A12)$$

and

$$\frac{d^2F_2}{d\eta^2} = -\frac{1}{4}\frac{f_2}{\sqrt{1+\eta_e}\cdot(1+\eta)^{3/2}} + \frac{df_2/d\eta}{\sqrt{(1+\eta_e)(1+\eta)}} + \sqrt{\frac{1+\eta}{1+\eta_e}}\cdot\frac{d^2f_2}{d\eta^2}$$

$$\frac{d^2f_2}{d\eta^2} = \frac{3}{4}\frac{1}{(1+\eta_e)^2}\cdot\left[1-\frac{5}{2}\left(\frac{\eta-\eta_e}{1+\eta_e}\right)\right] \qquad (A13)$$

First and second derivative of $C(\zeta,\eta)$, defined in section 2.1.2, are expressed by

$$\frac{dC}{d\eta} = \frac{\zeta^2}{4}\cdot\sqrt{\frac{1-\zeta}{1+\zeta/\zeta_1}}\cdot\frac{d}{d\eta}\left(\frac{1}{\zeta_1}\right)\cdot\left[1-\frac{3}{\zeta_1}\right] \qquad (A14)$$

$$\frac{d^2C}{d\eta^2} = -\frac{\zeta}{2}\cdot\frac{1}{(1+\zeta/\zeta_1)}\cdot\frac{d}{d\eta}\left(\frac{1}{\zeta_1}\right)\cdot\frac{dC}{d\eta} + \frac{\zeta^2}{4}\sqrt{\frac{1-\zeta}{1+\zeta/\zeta_1}}\cdot\left[\left(1-\frac{3}{\zeta_1}\right)\frac{d^2}{d\eta^2}\left(\frac{1}{\zeta_1}\right)-3\left(\frac{d}{d\eta}\left(\frac{1}{\zeta_1}\right)\right)^2\right] \qquad (A15)$$

Contd.

where

$$\frac{d}{d\eta}\left(\frac{1}{\zeta_1}\right) = \frac{d}{d\eta}\left(\frac{c_1}{c_2}\right) = \frac{1}{c_2}\left[\frac{dc_1}{d\eta} - \frac{1}{\zeta_1}\frac{dc_2}{d\eta}\right]$$

$$\frac{d^2}{d\eta^2}\left(\frac{1}{\zeta_1}\right) = -\frac{1}{c_2^2}\frac{dc_2}{d\eta}\left[\frac{dc_1}{d\eta} - \frac{1}{\zeta_1}\frac{dc_2}{d\eta}\right]$$

$$+\frac{1}{c_2}\left[\frac{d^2c_1}{d\eta^2} - \frac{d}{d\eta}\left(\frac{1}{\zeta_1}\right)\frac{dc_2}{d\eta} - \frac{1}{\zeta_1}\frac{d^2c_2}{d\eta^2}\right] \qquad \text{(A15) Contd.}$$

First and second derivative of $H(\eta)$, defined in section 2.2.2, are expressed by

$$\frac{dH}{d\eta} = \frac{1}{2\sqrt{1+\eta}} \cdot \left[-A\eta^3+B\eta^2-C\eta+D\right] + \sqrt{1+\eta}\ \left[-3A\eta^2+2B\eta-C\right]$$

for $-1 \leq \eta \leq -\eta_2$

$$= 0$$

for $\eta > -\eta_2$

$$\frac{d^2H}{d\eta^2} = \frac{-1}{4(1+\eta)^{3/2}} \cdot \left[-A\eta^3+B\eta^2-C\eta+D\right] + \frac{1}{\sqrt{1+\eta}} \cdot \left[-3A\eta^2+2B\eta-C\right] \qquad \text{(A16)}$$

$$+ \sqrt{1+\eta}\ \left[-6A\eta+2B\right]$$

for $-1 \leq \eta \leq -\eta_2$

$$= 0$$

for $\eta > -\eta_2$

The above expressions and equation (16) of section 3.2 are used in the evaluation of the coefficients of the log singularity terms (a_{p_i}, a_{q_i}).

TABLE 1

Generalised forces

The lift L, pitching moment M, hinge moment H and rolling moment B have been defined in section 4.4.1

L	M	H	B
0.6992	0.3935	0.0042	0.1861

TABLE 2

	ΔC_p at η stations			
$\bar{x}$	0.35	0.45	0.60	0.75
0.0125	1.276	1.712	2.973	4.732
0.025	0.976	1.300	2.207	3.434
0.05	0.654	0.919	1.643	2.530
0.1	0.444	0.686	1.326	1.965
0.2	0.495	0.742	1.333	1.681
0.3	0.493	0.801	1.492	1.626
0.4	0.527	0.963	1.807	1.634
0.5	0.692	1.395	2.348	1.606
0.575	0.827	2.008	2.992	1.499
0.625	0.901	2.797	3.714	1.357
0.64	0.925	3.170	4.040	1.302
0.6625	0.968	3.971	4.746	1.213
0.68	1.014	5.033	5.720	1.142
0.725	1.186	4.800	5.253	0.973
0.74	1.245	4.075	4.461	0.925
0.76	1.306	3.458	3.763	0.868
0.78	1.341	3.027	3.258	0.815
0.80	1.352	2.695	2.856	0.764
0.825	1.331	2.361	2.441	0.697
0.85	1.274	2.074	2.082	0.622
0.9	1.035	1.520	1.429	0.443
0.93	0.815	1.167	1.058	0.330
0.96	0.624	0.860	0.754	0.261
0.98	0.656	0.802	0.675	0.302

TABLE 3

	ΔC_p at η stations					
$\bar{x}$	0.19509	0.38268	0.55557	0.70711	0.83147	0.92388
0.0125	0.846	1.396	2.507	4.270	5.223	5.018
0.025	0.661	1.066	1.875	3.116	3.752	3.517
0.05	0.420	0.727	1.385	2.312	2.701	2.400
0.1	0.263	0.509	1.108	1.832	1.986	1.579
0.2	0.311	0.560	1.151	1.654	1.507	0.994
0.3	0.294	0.570	1.306	1.702	1.251	0.687
0.4	0.288	0.630	1.624	1.859	1.047	0.492
0.5	0.354	0.849	2.212	2.094	0.855	0.380
0.575	0.385	1.071	2.908	2.360	0.710	0.313
0.625	0.381	1.263	3.667	2.634	0.620	0.266
0.64	0.377	1.338	4.005	2.737	0.595	0.252
0.6625	0.372	1.474	4.729	2.890	0.560	0.231
0.68	0.370	1.609	5.717	2.911	0.535	0.216
0.725	0.378	2.155	5.290	1.979	0.478	0.182
0.74	0.386	2.197	4.511	1.776	0.462	0.173
0.76	0.401	2.139	3.832	1.562	0.441	0.163
0.78	0.420	2.034	3.344	1.392	0.421	0.155
0.8	0.440	1.918	2.959	1.249	0.400	0.148
0.825	0.460	1.772	2.562	1.092	0.372	0.141
0.85	0.465	1.618	2.214	0.945	0.339	0.132
0.9	0.391	1.245	1.563	0.650	0.252	0.097
0.93	0.292	0.969	1.175	0.476	0.196	0.066
0.96	0.242	0.728	0.845	0.354	0.175	0.057
0.98	0.390	0.724	0.756	0.370	0.236	0.115

TABLE 4

Integrated effects

$\frac{c\,C_{LL}}{\bar{c}\,C_L}$, X_{cp} , $\frac{c_\delta^2\,C_{HL}}{\bar{c}_\delta^2\,C_H}$ have been defined in section 4.4.1

η	$\frac{c\,C_{LL}}{\bar{c}\,C_L}$	X_{cp}	$\frac{c_\delta^2\,C_{HL}}{\bar{c}_\delta^2\,C_H}$
0.19509	0.4559	0.5063	
0.35	0.8663	0.5641	
0.38268	1.1009	0.5839	
0.4	1.3274	0.5976	0.5976
0.45	1.7825	0.5993	0.6371
0.5	1.9735	0.5832	0.6100
0.55556	2.0546	0.5614	0.5388
0.6	2.0374	0.5415	0.4585
0.65	1.9086	0.5122	0.3370
0.7	1.4998	0.4467	0.1798
0.7071	1.3883	0.4265	
0.75	1.0567	0.3569	
0.83147	0.7174	0.2525	
0.92388	0.4110	0.2095	

TEST CASE WING PLANFORM

$\Lambda = 45°$
$\lambda = 1$
$A = 4$

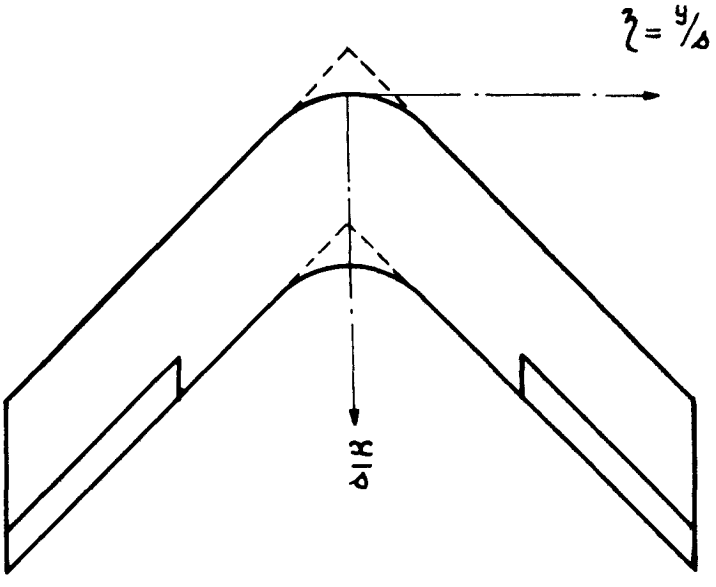

FIG. 1B

WING A

$\Lambda_{1/2} = 30°$
$\lambda = 1/3$
$A = 6$

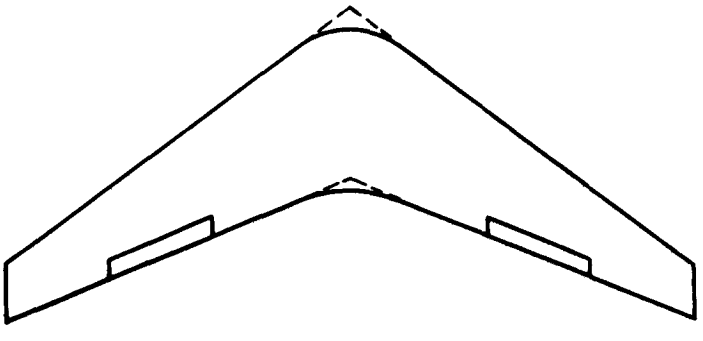

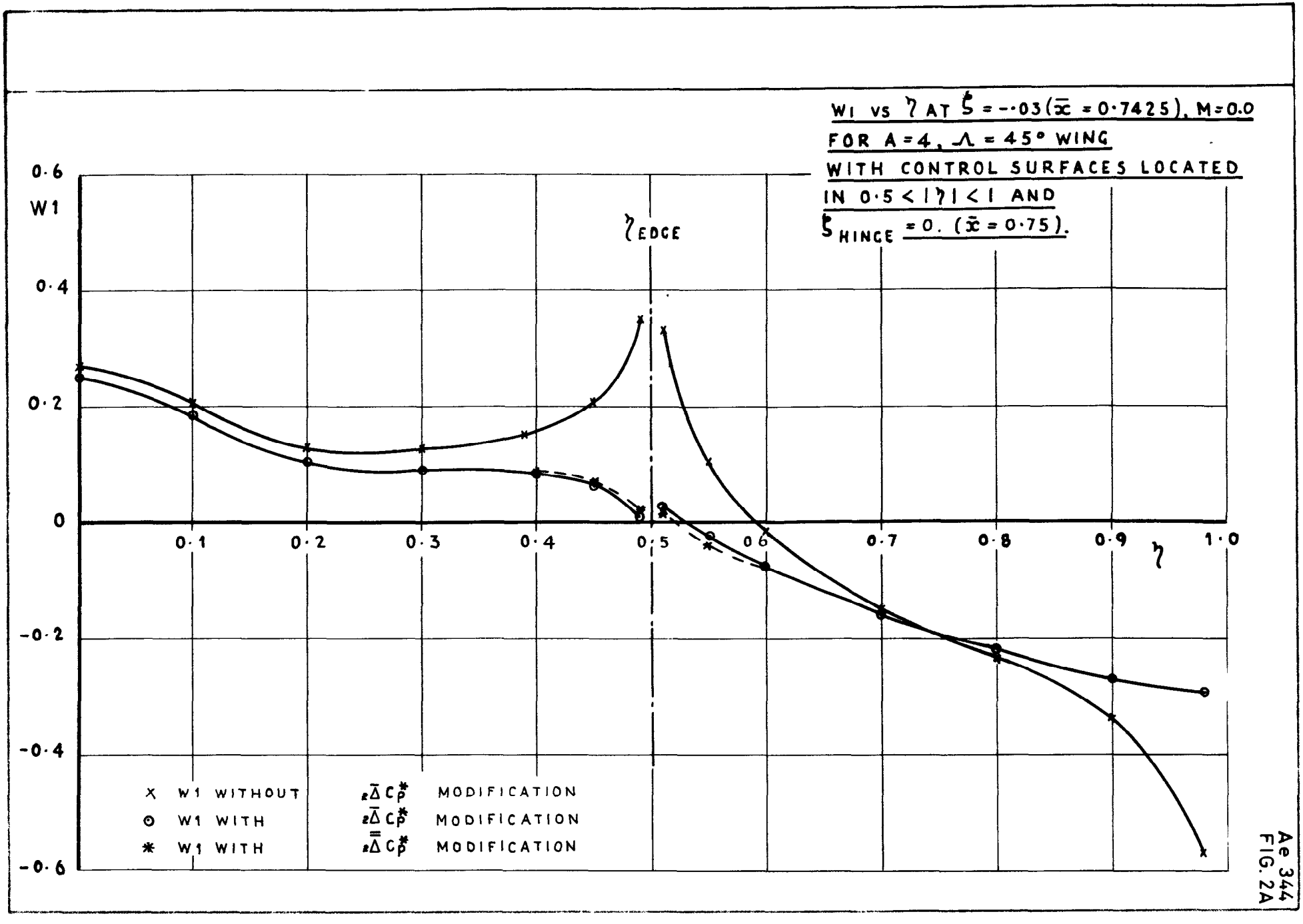
W1 VS η AT ξ = -·03 (x̄ = 0·7425), M=0·0
FOR A=4, Λ = 45° WING
WITH CONTROL SURFACES LOCATED
IN 0·5 < |η| < 1 AND
ξ HINGE = 0. (x̄ = 0·75).
W1
0·6
0·4
0·2
0
-0·2
-0·4
-0·6
η EDGE
0·1
0·2
0·3
0·4
0·5
0·6
0·7
0·8
0·9
1·0
η
× W1 WITHOUT
⊙ W1 WITH
✱ W1 WITH
MODIFICATION
MODIFICATION
MODIFICATION

Ae 344
FIG. 2A

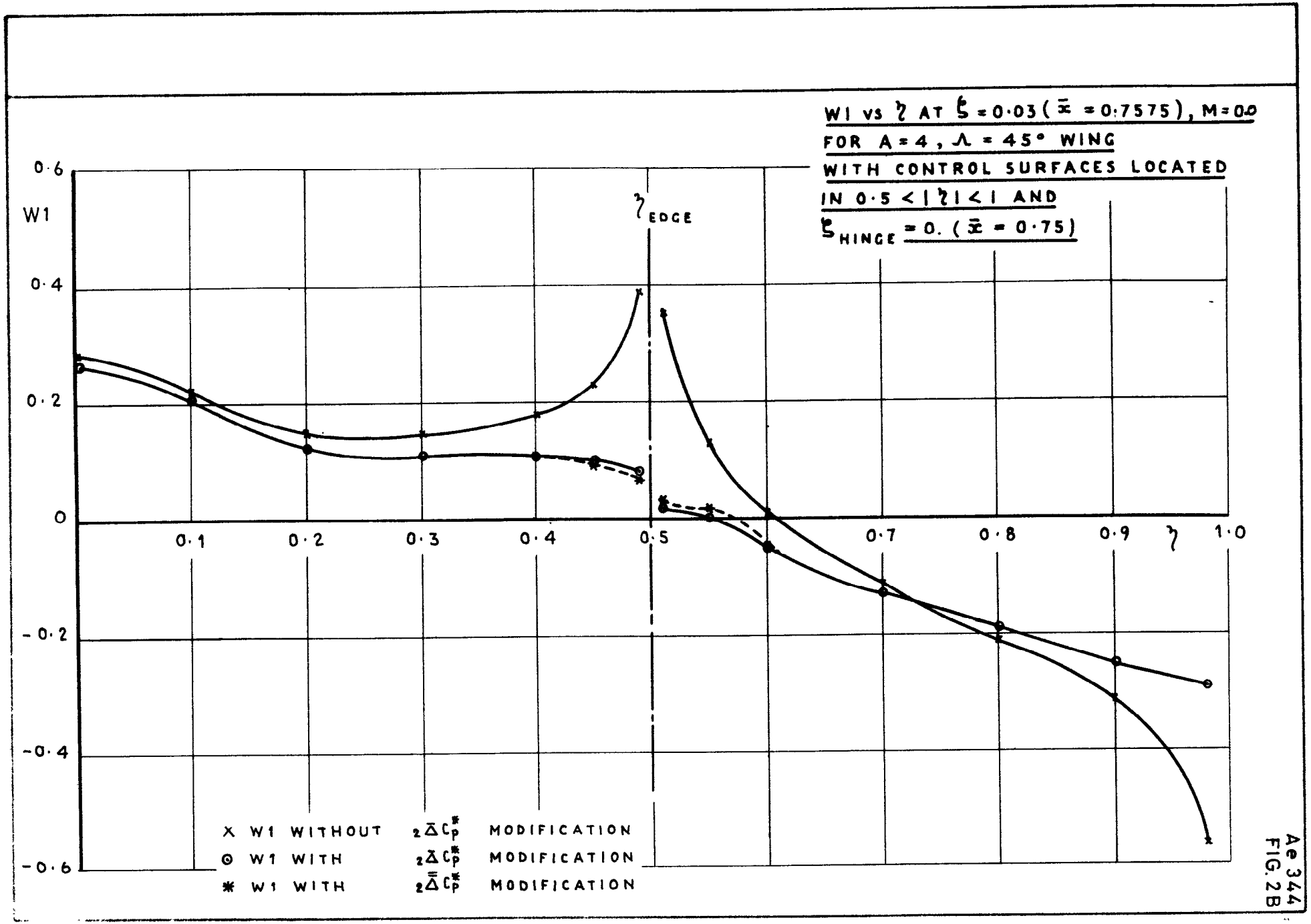
W1 vs η AT ξ = 0·03 (x̄ = 0·7575), M = 0·0
FOR A = 4 , Λ = 45° WING
WITH CONTROL SURFACES LOCATED
IN 0·5 < |η| < 1 AND
ξ HINGE = 0. (x̄ = 0·75)
W1
η EDGE
η
0·6
0·4
0·2
0
-0·2
-0·4
-0·6
0·1
0·2
0·3
0·4
0·5
0·7
0·8
0·9
1·0
X W1 WITHOUT 2Δ̄Cp* MODIFICATION
⊙ W1 WITH 2Δ̄Cp* MODIFICATION
* W1 WITH 2Δ̄Cp* MODIFICATION

Ae 344
FIG. 2B

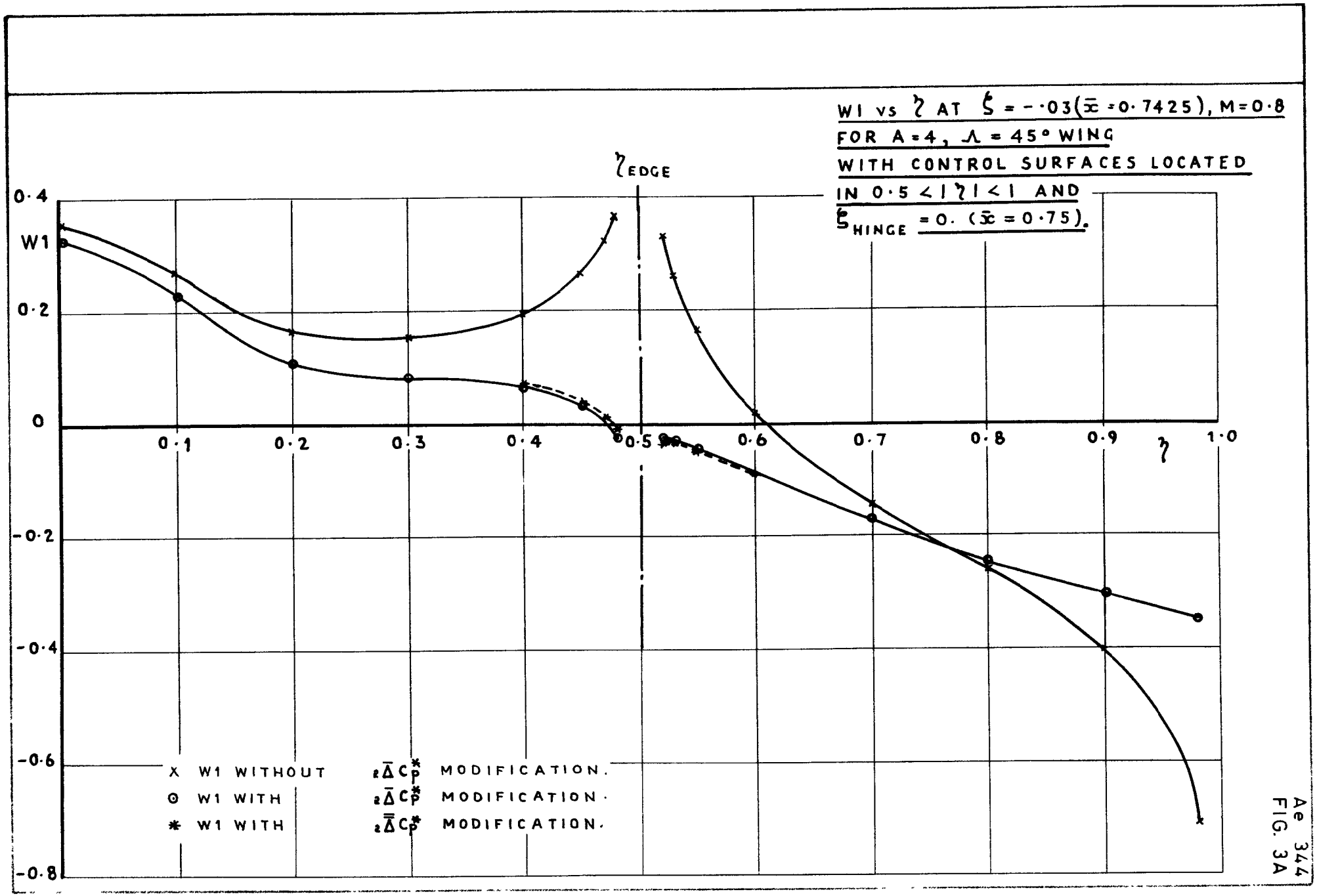
W1 vs η AT ξ = -·03(x̄ = 0·7425), M=0·8
FOR A=4, Λ = 45° WING
WITH CONTROL SURFACES LOCATED
IN 0·5 < |η| < 1 AND
ξ HINGE = 0. (x̄ = 0·75).
η EDGE
W1
0·4
0·2
0
-0·2
-0·4
-0·6
-0·8
0·1
0·2
0·3
0·4
0·5
0·6
0·7
0·8
0·9
1·0
η
X W1 WITHOUT 2Δ̄Cp* MODIFICATION.
⊙ W1 WITH 2Δ̄Cp* MODIFICATION.
* W1 WITH 2Δ̄Cp* MODIFICATION.

Ae 344
FIG. 3A

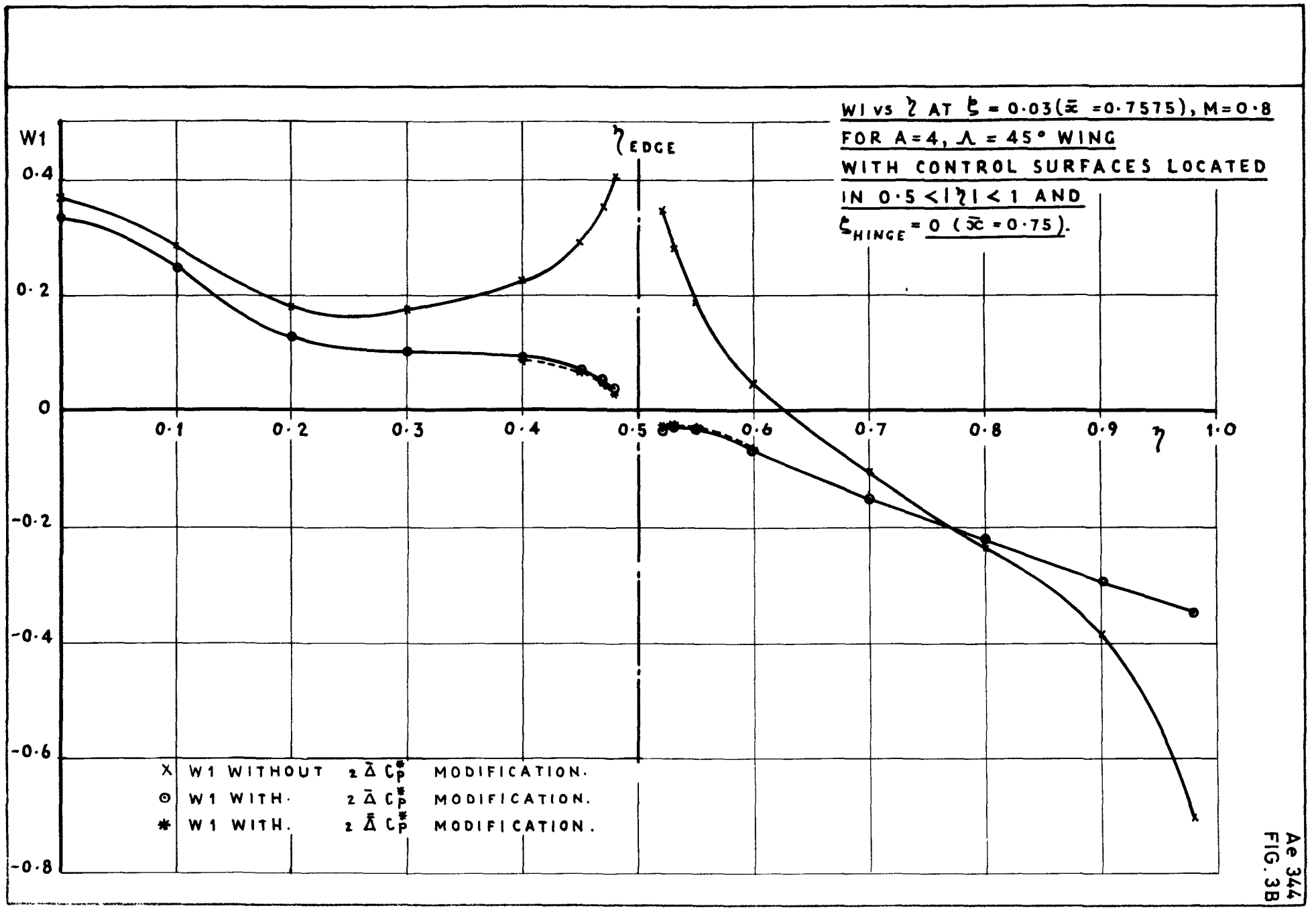
W1 vs η AT ξ = 0·03 (x̄ = 0·7575), M = 0·8
FOR A = 4, Λ = 45° WING
WITH CONTROL SURFACES LOCATED
IN 0·5 < |η| < 1 AND
ξ HINGE = 0 (x̄ = 0·75).
W1
0·4
0·2
0
-0·2
-0·4
-0·6
-0·8
0·1
0·2
0·3
0·4
0·5
0·6
0·7
0·8
0·9
1·0
η
η EDGE
X W1 WITHOUT 2 Δ̄ Cp* MODIFICATION.
⊙ W1 WITH 2 Δ̄ Cp* MODIFICATION.
* W1 WITH. 2 Δ̄ Cp* MODIFICATION.

Ae 344
FIG. 3B

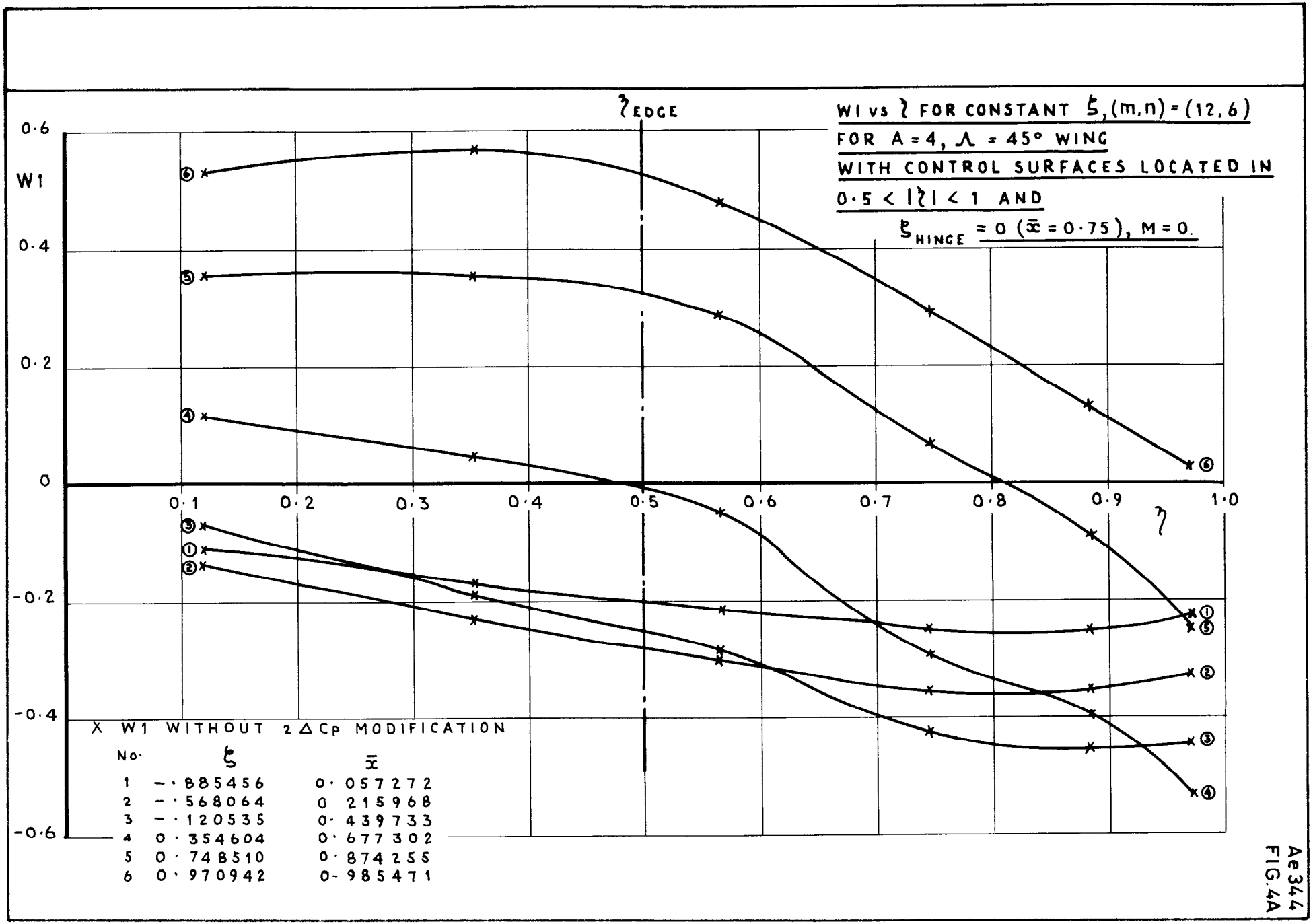
W1 vs η FOR CONSTANT ξ, (m,n) = (12,6)
FOR A = 4, Λ = 45° WING
WITH CONTROL SURFACES LOCATED IN
0·5 < |η| < 1 AND
ξ HINGE = 0 (x̄ = 0·75), M = 0.
η EDGE
W1
0·6
0·4
0·2
0
-0·2
-0·4
-0·6
0·1
0·2
0·3
0·4
0·5
0·6
0·7
0·8
0·9
1·0
η
X W1 WITHOUT 2 Δ Cp MODIFICATION
No. ξ x̄
1 −·885456 0·057272
2 −·568064 0 215968
3 −·120535 0·439733
4 0·354604 0·677302
5 0·748510 0·874255
6 0·970942 0-985471

Ae344
FIG.4A

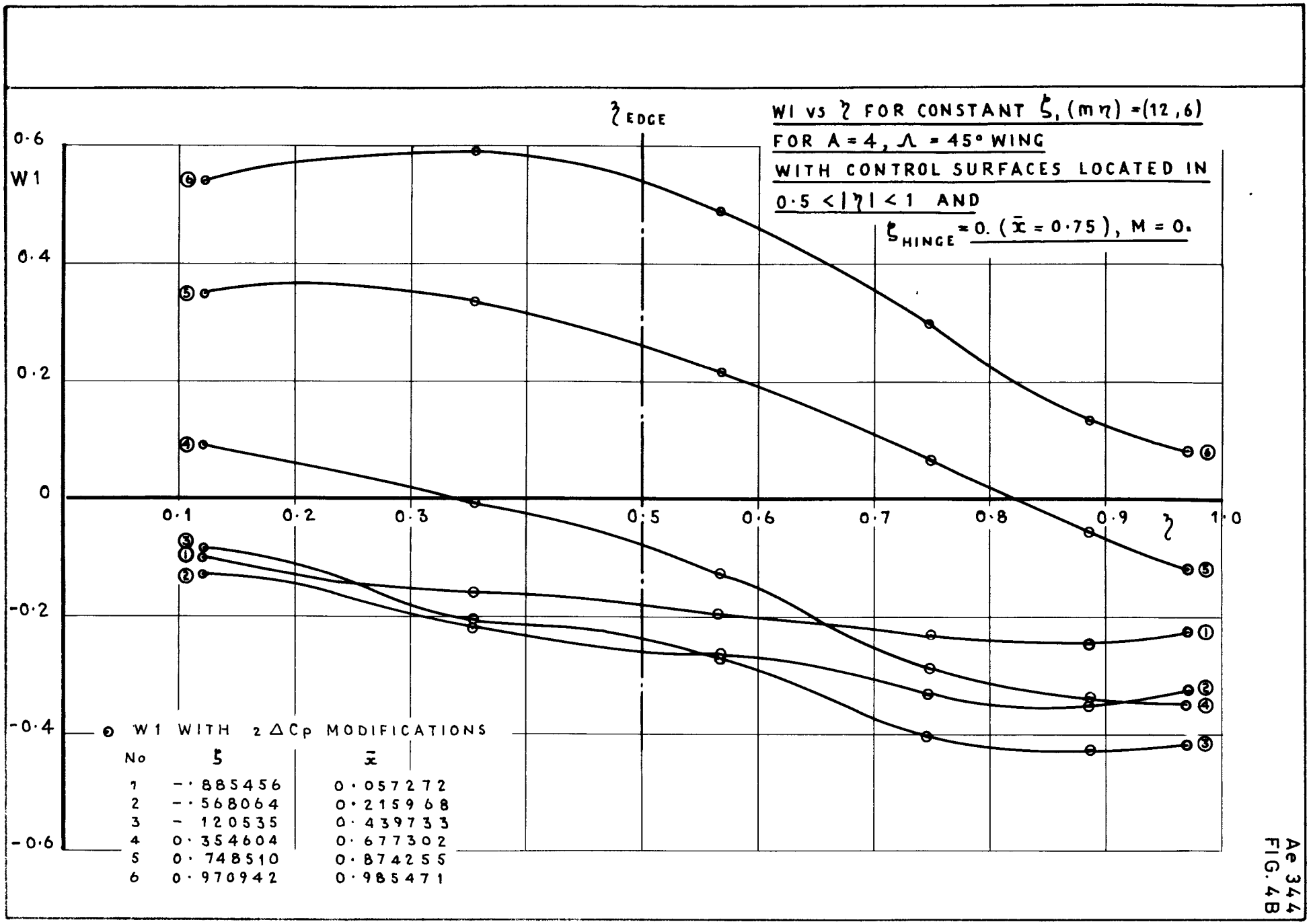
WI vs η FOR CONSTANT ξ, (mη) =(12,6)
FOR A = 4, Λ = 45° WING
WITH CONTROL SURFACES LOCATED IN
0·5 < |η| < 1 AND
ξ HINGE = 0. (x̄ = 0·75), M = 0.
η EDGE
W1
0·6
0·4
0·2
0
-0·2
-0·4
-0·6
0·1
0·2
0·3
0·5
0·6
0·7
0·8
0·9
1·0
η
⊙ W1 WITH 2 ΔCp MODIFICATIONS
No ξ x̄
1 −·885456 0·057272
2 −·568064 0·215968
3 −·120535 0·439733
4 0·354604 0·677302
5 0·748510 0·874255
6 0·970942 0·985471
Ae 344
FIG. 4B

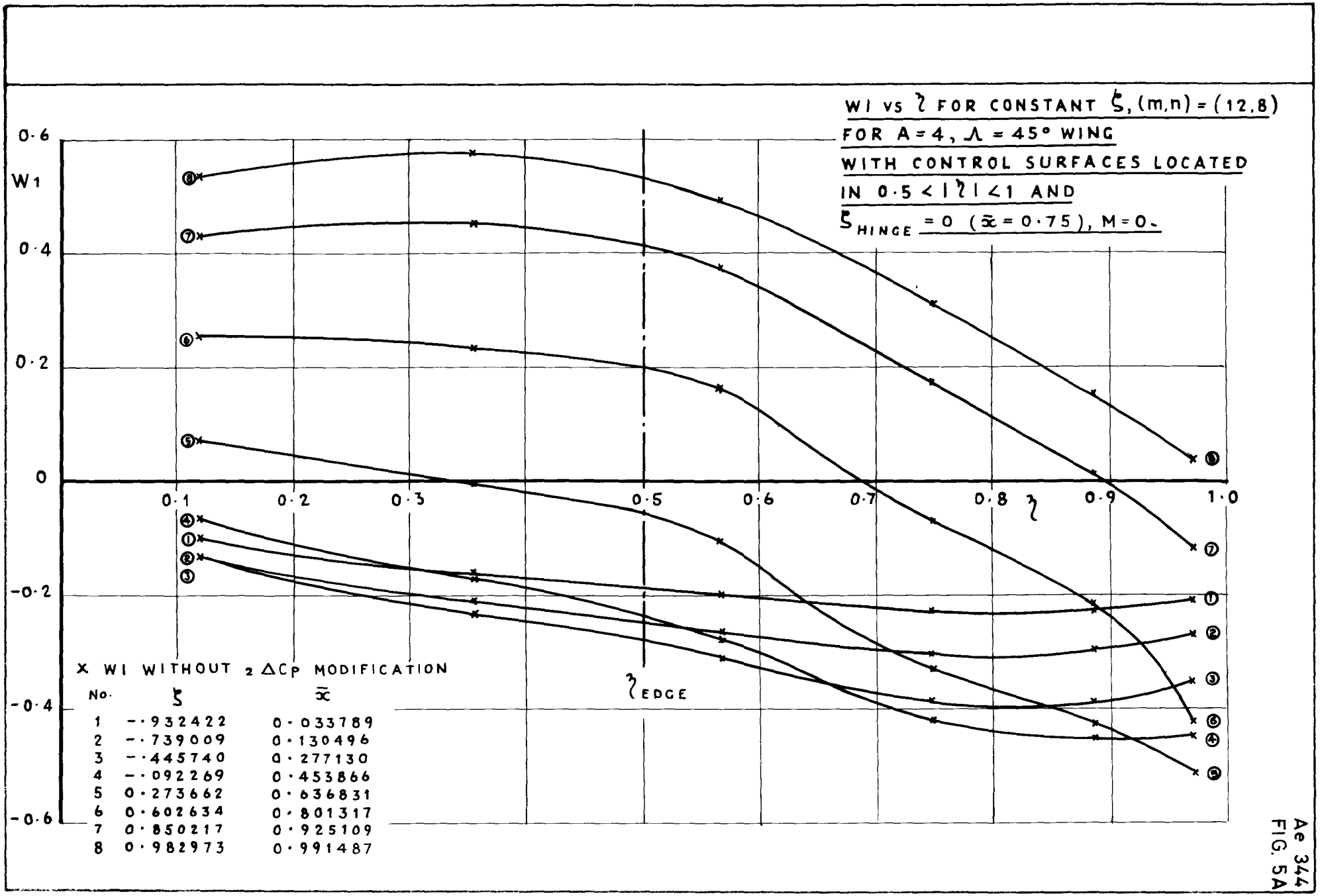
WI vs η FOR CONSTANT ξ, (m,n) = (12,8)
FOR A = 4, Λ = 45° WING
WITH CONTROL SURFACES LOCATED
IN 0.5 < |η| < 1 AND
ξ HINGE = 0 (x̄ = 0.75), M = 0.
0·6
WI
0·4
0·2
0
-0·2
-0·4
-0·6
0·1
0·2
0·3
0·5
0·6
0·7
0·8
η
0·9
1·0
η EDGE
X WI WITHOUT 2 ΔCp MODIFICATION
No. ξ x̄
1 -·932422 0·033789
2 -·739009 0·130496
3 -·445740 0·277130
4 -·092269 0·453866
5 0·273662 0·636831
6 0·602634 0·801317
7 0·850217 0·925109
8 0·982973 0·991487

Ae 344
FIG. 5A

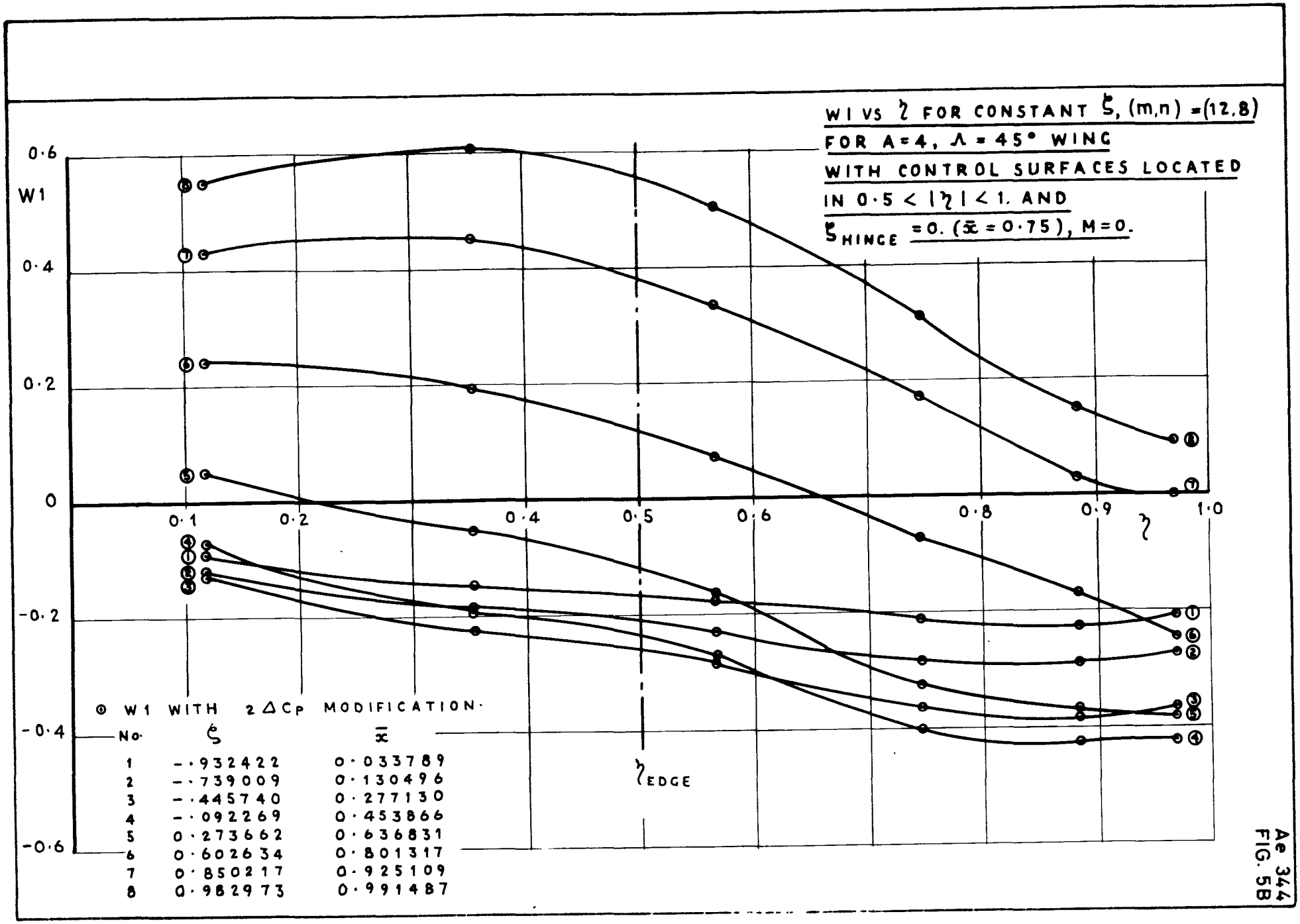
W1 VS η FOR CONSTANT ξ, (m,n) =(12,8)
FOR A=4, Λ = 45° WING
WITH CONTROL SURFACES LOCATED
IN 0·5 < |η| < 1. AND
ξ HINGE =0. (x̄ = 0·75), M=0.
W1
0·6
0·4
0·2
0
-0·2
-0·4
-0·6
0·1
0·2
0·4
0·5
0·6
0·8
0·9
1·0
η
η EDGE
⊙ W1 WITH 2ΔCp MODIFICATION·
No. ξ x̄
1 −·932422 0·033789
2 −·739009 0·130496
3 −·445740 0·277130
4 −·092269 0·453866
5 0·273662 0·636831
6 0·602634 0·801317
7 0·850217 0·925109
8 0·982973 0·991487

Ae 344
FIG. 5B

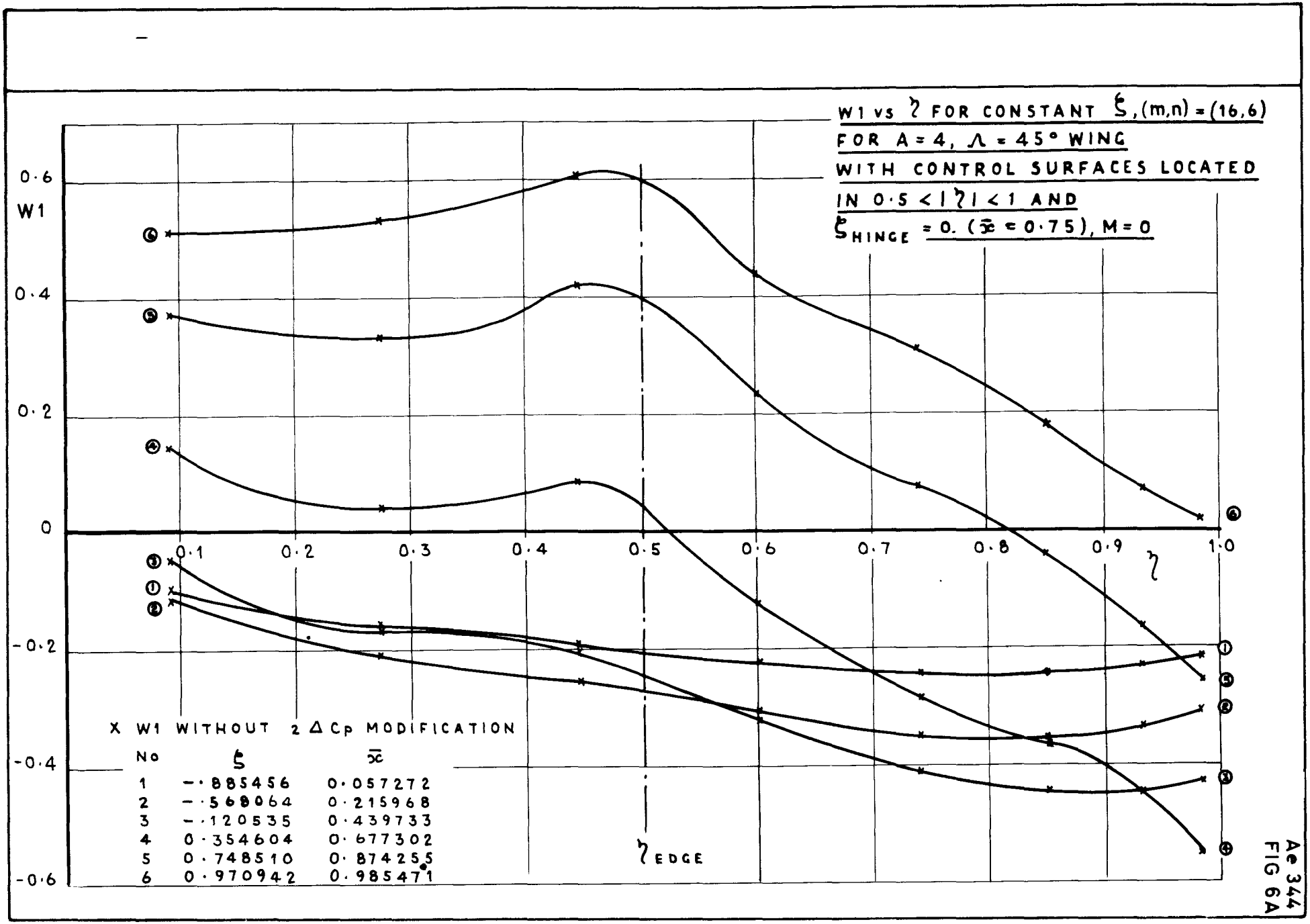
W1 vs η FOR CONSTANT ξ, (m,n) = (16,6)
FOR A = 4, Λ = 45° WING
WITH CONTROL SURFACES LOCATED
IN 0·5 < |η| < 1 AND
ξ HINGE = 0. (x̄ = 0·75), M = 0
W1
0·6
0·4
0·2
0
-0·2
-0·4
-0·6
0·1
0·2
0·3
0·4
0·5
0·6
0·7
0·8
0·9
1·0
η
η EDGE
X W1 WITHOUT 2 Δ Cp MODIFICATION
No ξ x̄
1 −·885456 0·057272
2 −·568064 0·215968
3 −·120535 0·439733
4 0·354604 0·677302
5 0·748510 0·874255
6 0·970942 0·985471

Ae 344
FIG 6A

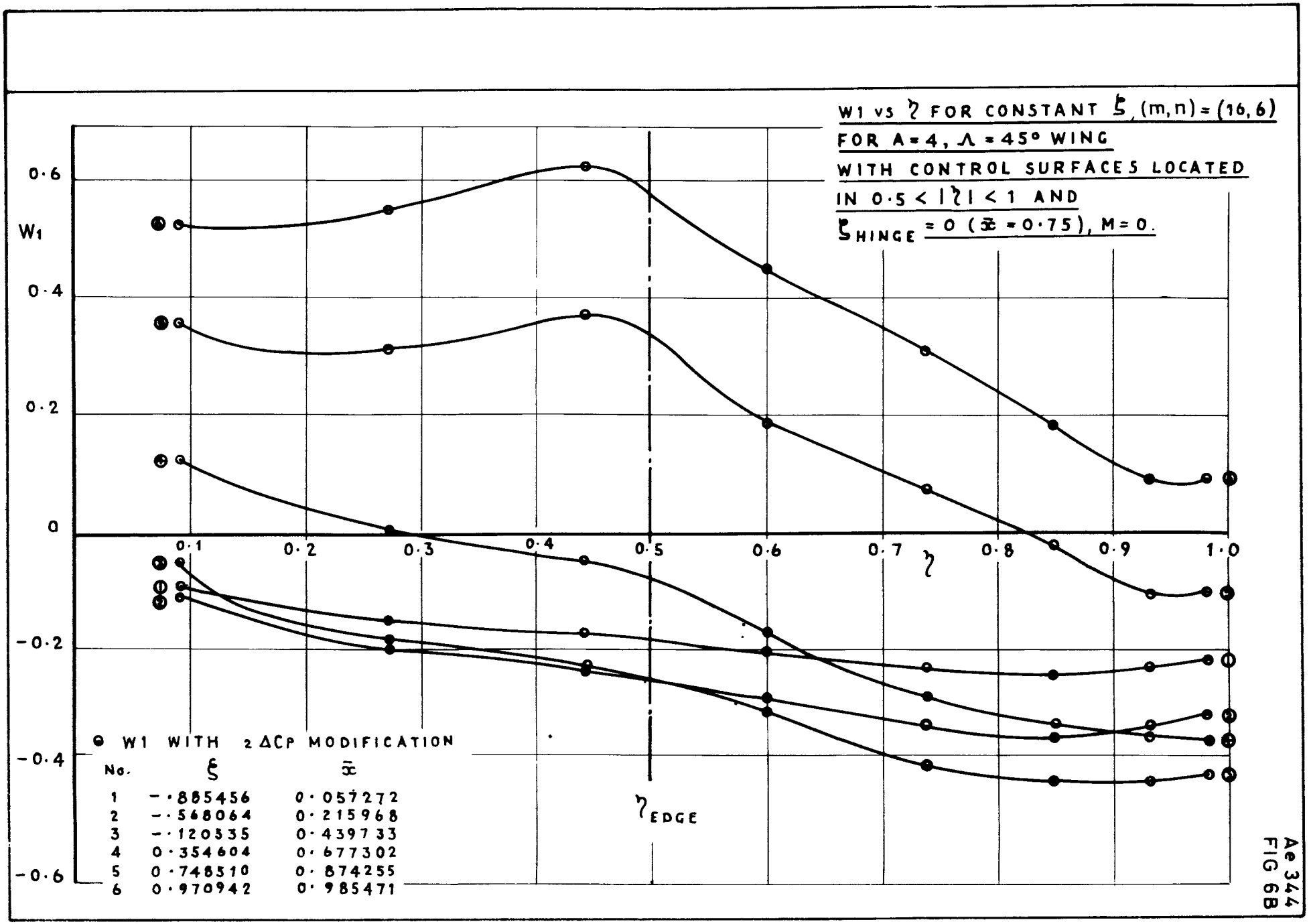
W1 vs η FOR CONSTANT ξ, (m,n) = (16,6)
FOR A = 4, Λ = 45° WING
WITH CONTROL SURFACES LOCATED
IN 0·5 < |η| < 1 AND
ξ HINGE = 0 (x̄ = 0·75), M = 0.
W1
0·6
0·4
0·2
0
-0·2
-0·4
-0·6
0·1
0·2
0·3
0·4
0·5
0·6
0·7
0·8
0·9
1·0
η
η EDGE
⊖ W1 WITH 2 ΔCp MODIFICATION
No. ξ x̄
1 −·885456 0·057272
2 −·568064 0·215968
3 −·120535 0·439733
4 0·354604 0·677302
5 0·748510 0·874255
6 0·970942 0·985471
Ae 344
FIG 6B

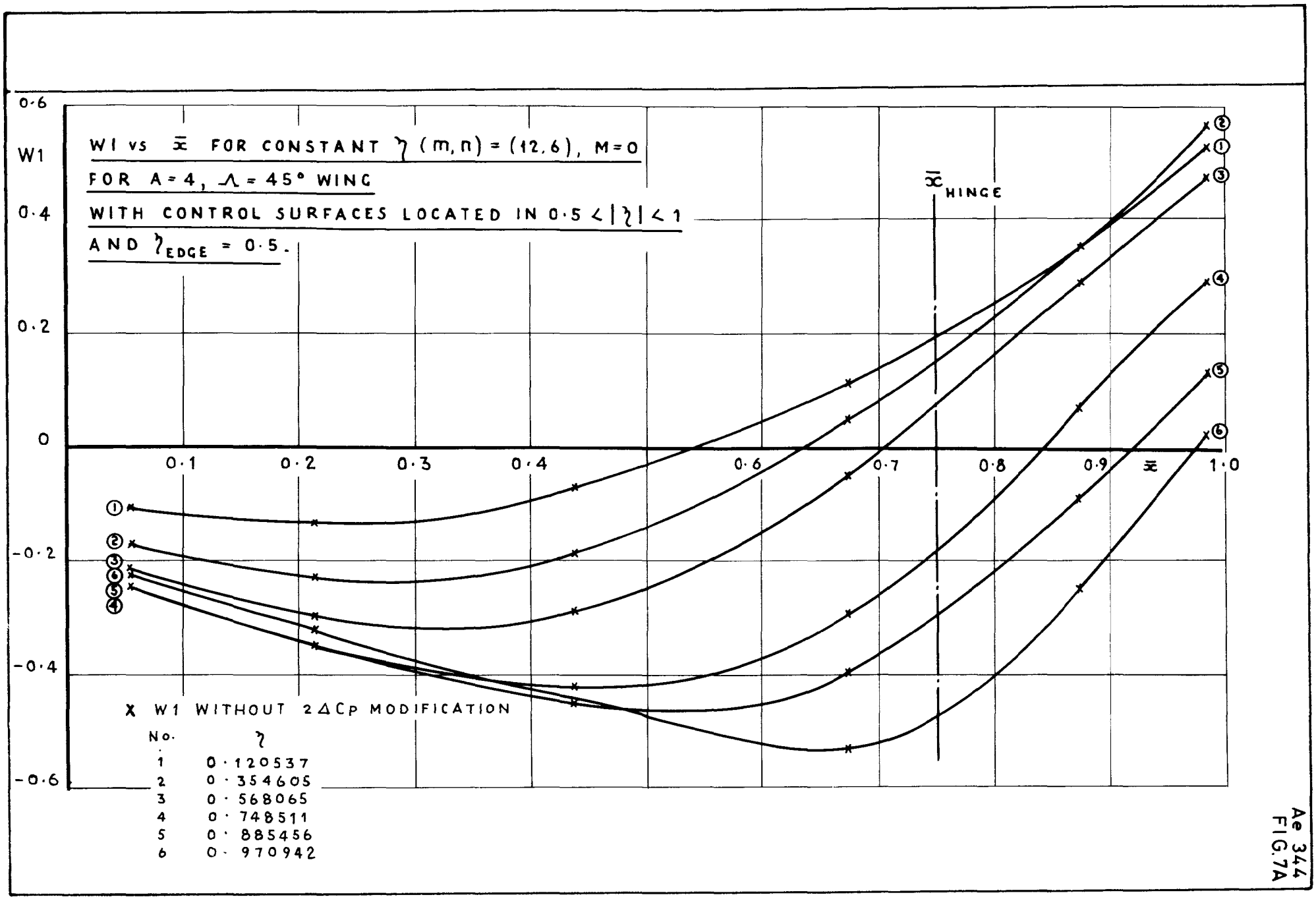
W1 vs $\bar{x}$ FOR CONSTANT η (m,n) = (12,6), M=0
FOR A=4, Λ = 45° WING
WITH CONTROL SURFACES LOCATED IN 0·5 < |η| < 1
AND η_{EDGE} = 0·5.
$\bar{x}_{HINGE}$
W1
$\bar{x}$
0·6
0·4
0·2
0
-0·2
-0·4
-0·6
0·1
0·2
0·3
0·4
0·6
0·7
0·8
0·9
1·0
X W1 WITHOUT 2ΔCp MODIFICATION
No. η
1 0·120537
2 0·354605
3 0·568065
4 0·748511
5 0·885456
6 0·970942

Ae 344
FIG.7A

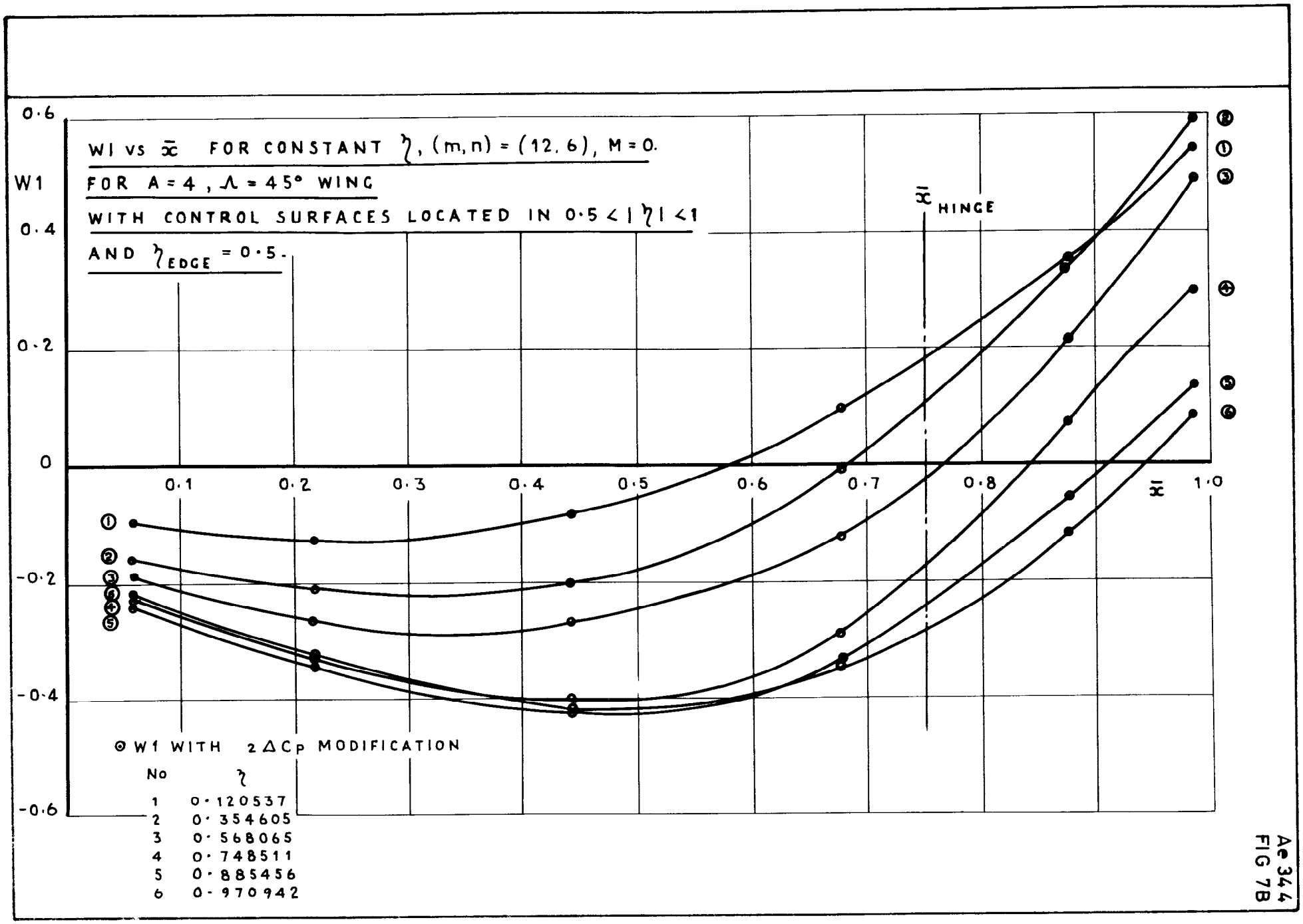
W1 vs $\bar{x}$ FOR CONSTANT η, (m,n) = (12, 6), M = 0.
FOR A = 4, Λ = 45° WING
WITH CONTROL SURFACES LOCATED IN 0·5 < |η| < 1
AND η_{EDGE} = 0·5.
W1
0·6
0·4
0·2
0
-0·2
-0·4
-0·6
0·1
0·2
0·3
0·4
0·5
0·6
0·7
0·8
1·0
$\bar{x}$
$\bar{x}$ HINGE
① ② ③ ④ ⑤ ⑥
⊙ W1 WITH 2ΔCp MODIFICATION
No η
1 0·120537
2 0·354605
3 0·568065
4 0·748511
5 0·885456
6 0·970942
Ae 344
FIG 7B

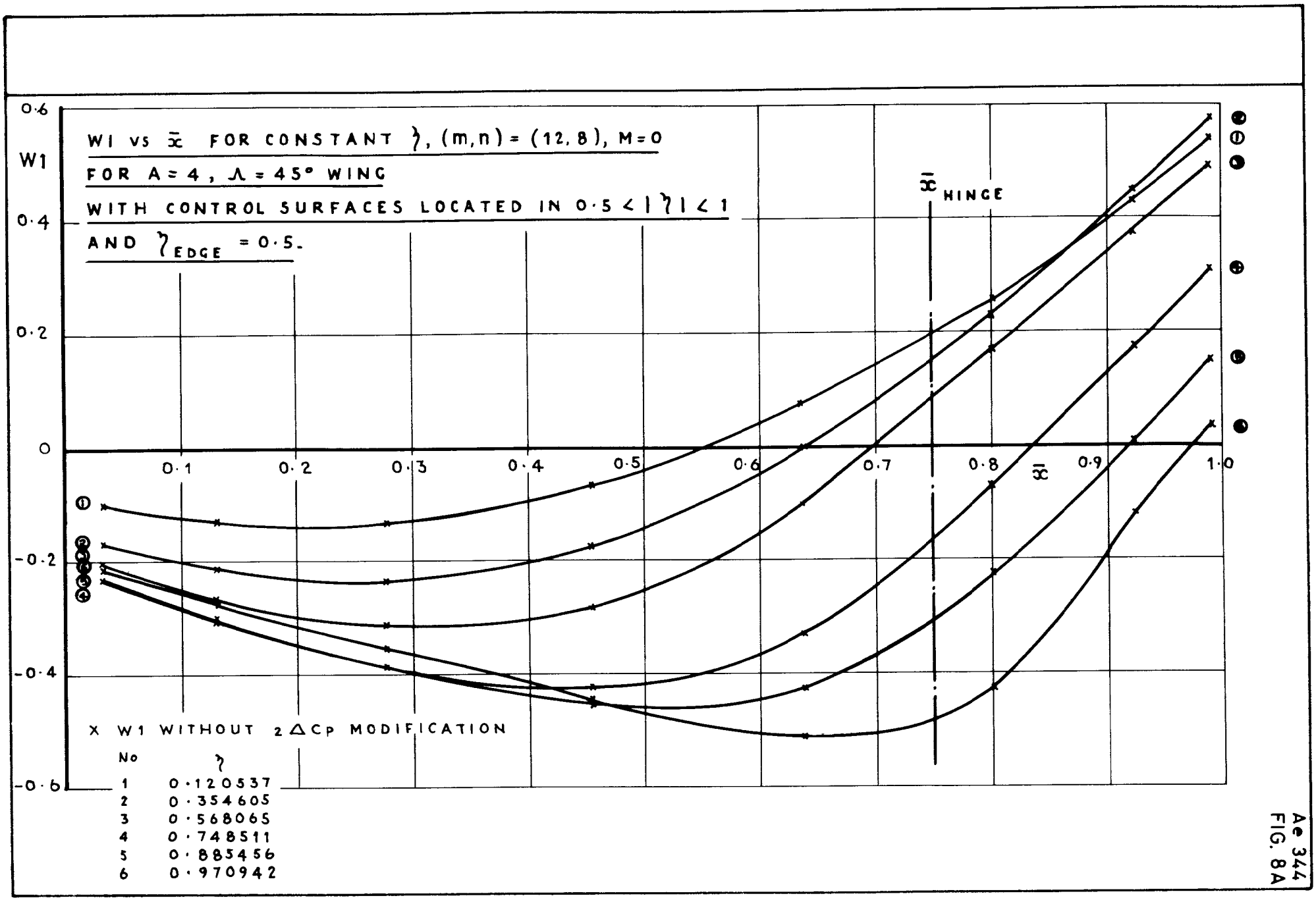
W1 vs $\bar{x}$ FOR CONSTANT η, (m,n) = (12, 8), M = 0
FOR A = 4, Λ = 45° WING
WITH CONTROL SURFACES LOCATED IN 0·5 < |η| < 1
AND η_{EDGE} = 0·5.
W1
0·6
0·4
0·2
0
-0·2
-0·4
-0·6
0·1
0·2
0·3
0·4
0·5
0·6
0·7
0·8
0·9
1·0
$\bar{x}$
$\bar{x}$ HINGE
X W1 WITHOUT 2ΔCp MODIFICATION
No η
1 0·120537
2 0·354605
3 0·568065
4 0·748511
5 0·885456
6 0·970942

Ae 344
FIG. 8A

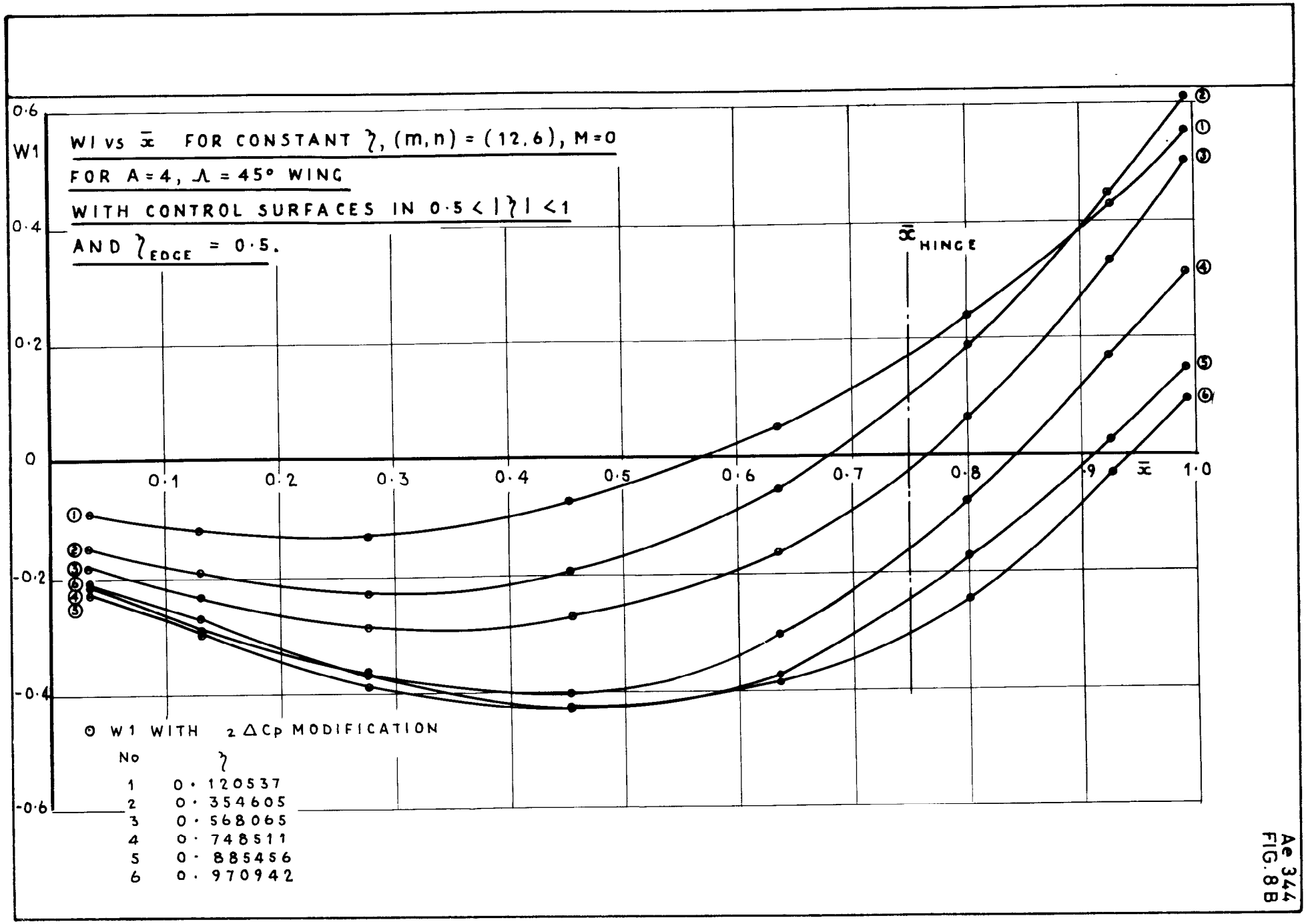
W1 vs $\bar{x}$ FOR CONSTANT η, (m,n) = (12,6), M=0
FOR A=4, Λ = 45° WING
WITH CONTROL SURFACES IN $0.5 < |\eta| < 1$
AND η_{EDGE} = 0.5.
$\bar{x}_{HINGE}$
W1
$\bar{x}$
0.6
0.4
0.2
0
-0.2
-0.4
-0.6
0.1
0.2
0.3
0.4
0.5
0.6
0.7
0.8
.9
1.0
① ② ③ ④ ⑤ ⑥
⊙ W1 WITH 2 ΔCp MODIFICATION
No η
1 0.120537
2 0.354605
3 0.568065
4 0.748511
5 0.885456
6 0.970942

Ae 344
FIG. 8B

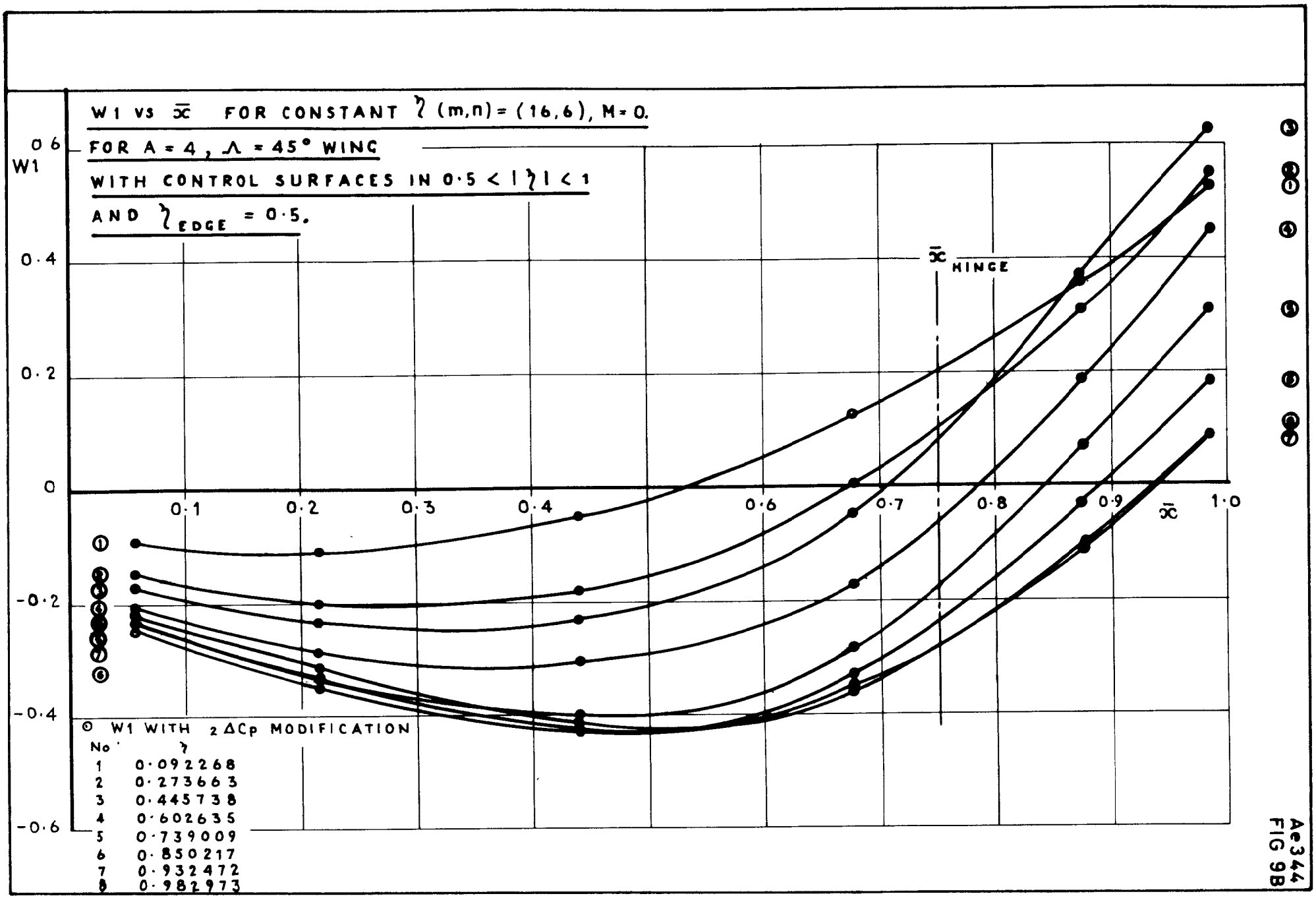
W1 vs $\bar{x}$ FOR CONSTANT η (m,n) = (16,6), M = 0.
FOR A = 4, Λ = 45° WING
WITH CONTROL SURFACES IN 0·5 < |η| < 1
AND η_{EDGE} = 0·5.
W1
0·6
0·4
0·2
0
-0·2
-0·4
-0·6
0·1
0·2
0·3
0·4
0·6
0·7
0·8
0·9
1·0
$\bar{x}$
$\bar{x}_{HINGE}$
① W1 WITH $_2\Delta C_p$ MODIFICATION
No η
1 0·092268
2 0·273663
3 0·445738
4 0·602635
5 0·739009
6 0·850217
7 0·932472
8 0·982973

Ae344
FIG 9B

ERROR FUNCTION VS η FOR CONSTANT ξ

$(m,n) = (16,6)$, $A = 4$, $\Lambda = 45°$, $M = 0$

CONTROL SURFACES LOCATED IN $0.5 < |\eta| < 1$

$\xi_{HINGE} = 0$ $(\bar{x} = 0.75)$.

$\bar{x} = 0.677302$

X $E = W_1 - W_1^{INT}$

● $E = W_1^* - W_1^{*\,INT.}$

INT=INTERPOLATED

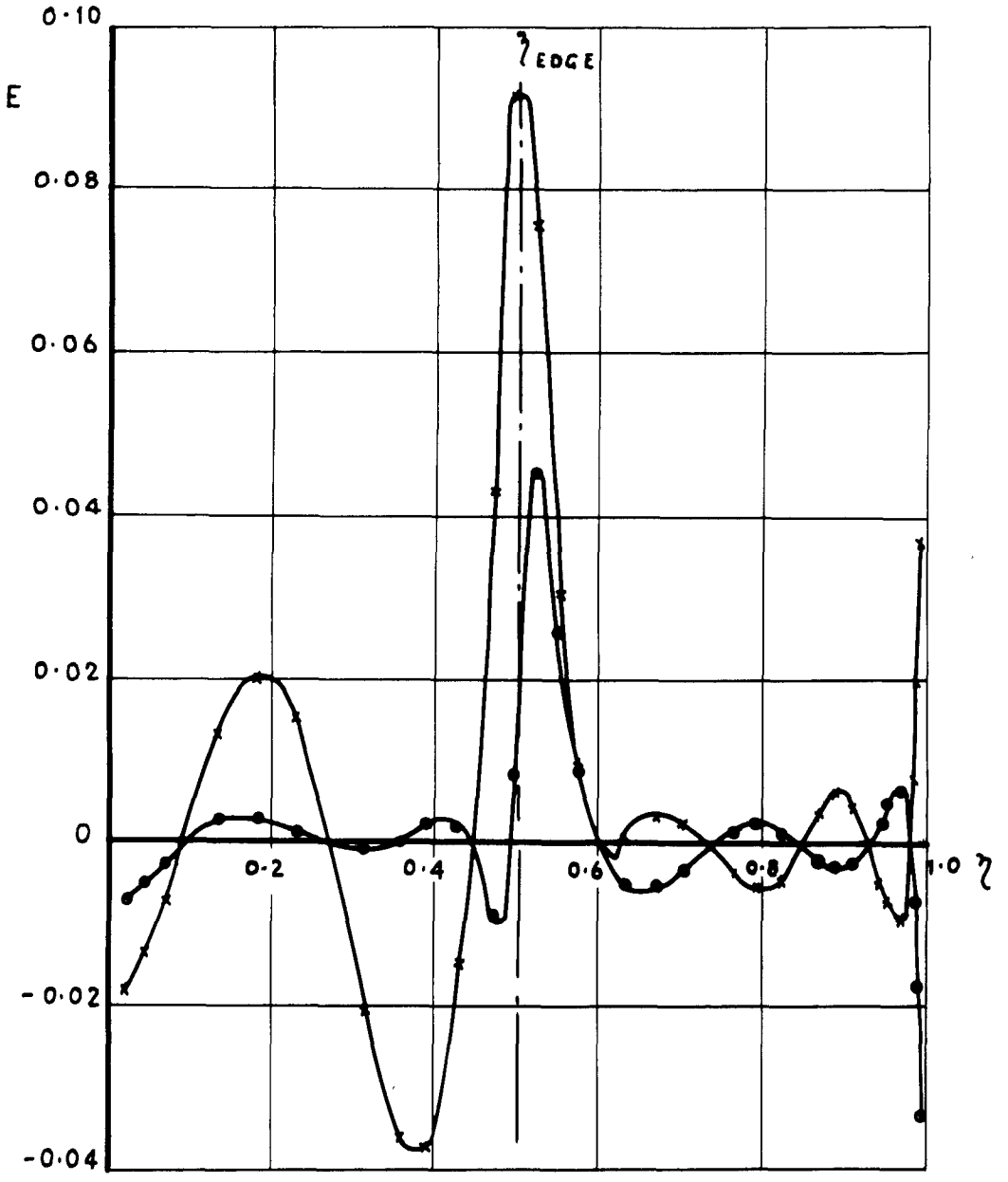

ERROR FUNCTION VS η FOR CONSTANT ξ

$(m,n) = (16,6)$, $A = 4$, $\Lambda = 45°$, $M = 0$

CONTROL SURFACES LOCATED IN $0.5 < |\eta| < 1$

$\xi_{HINGE} = 0$ $(\bar{x} = 0.75)$.

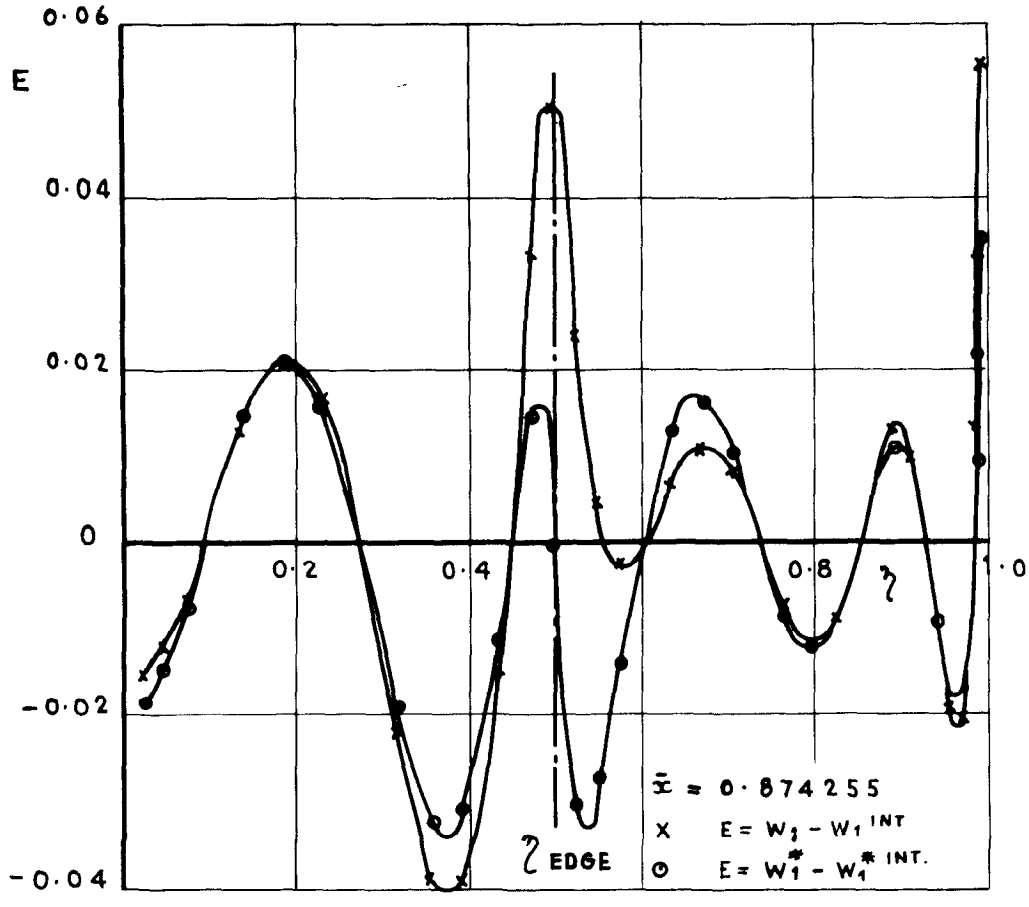

FIG. 12

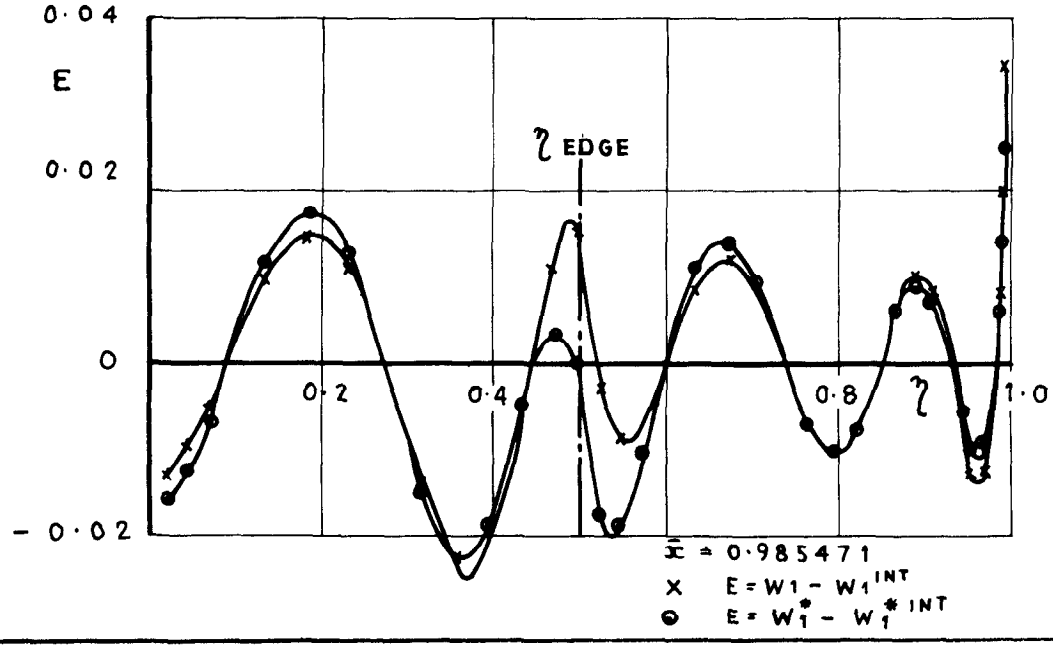

ERROR FUNCTION VS $\bar{x}$ FOR CONSTANT η

$(m,n) = (16,6)$, $A = 4$, $\Lambda = 45°$, $M = 0$

CONTROL SURFACES LOCATED IN $0.5 < |\eta| < 1$

$\zeta_{HINGE} = 0$ $(\bar{x} = 0.75)$

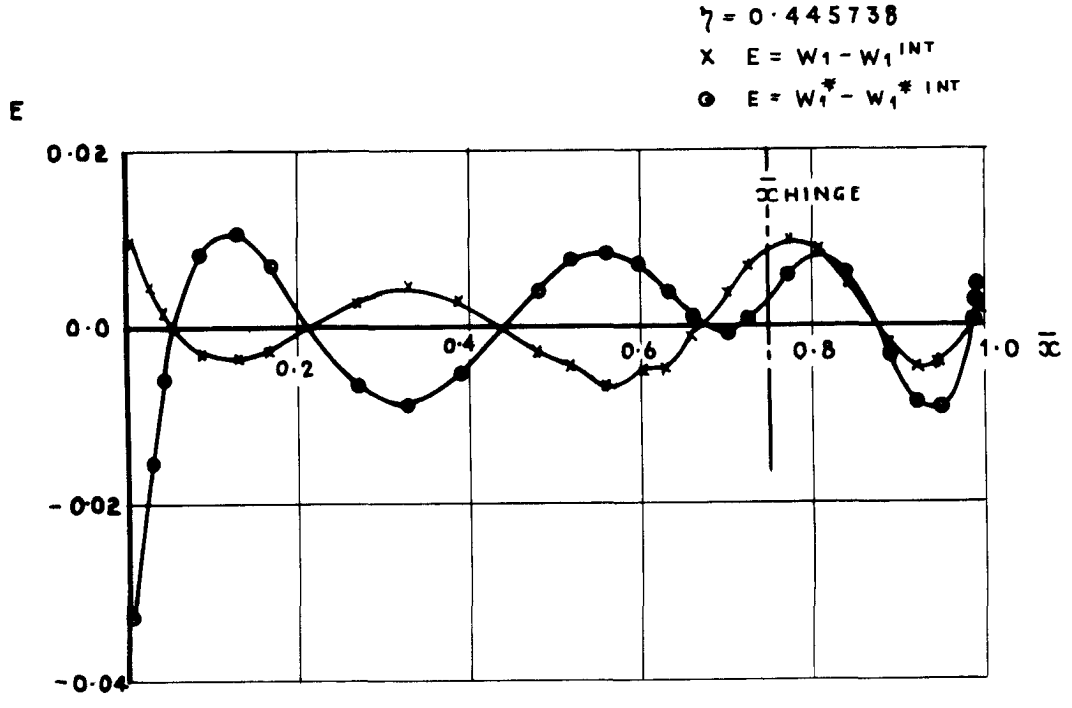

FIG. 14

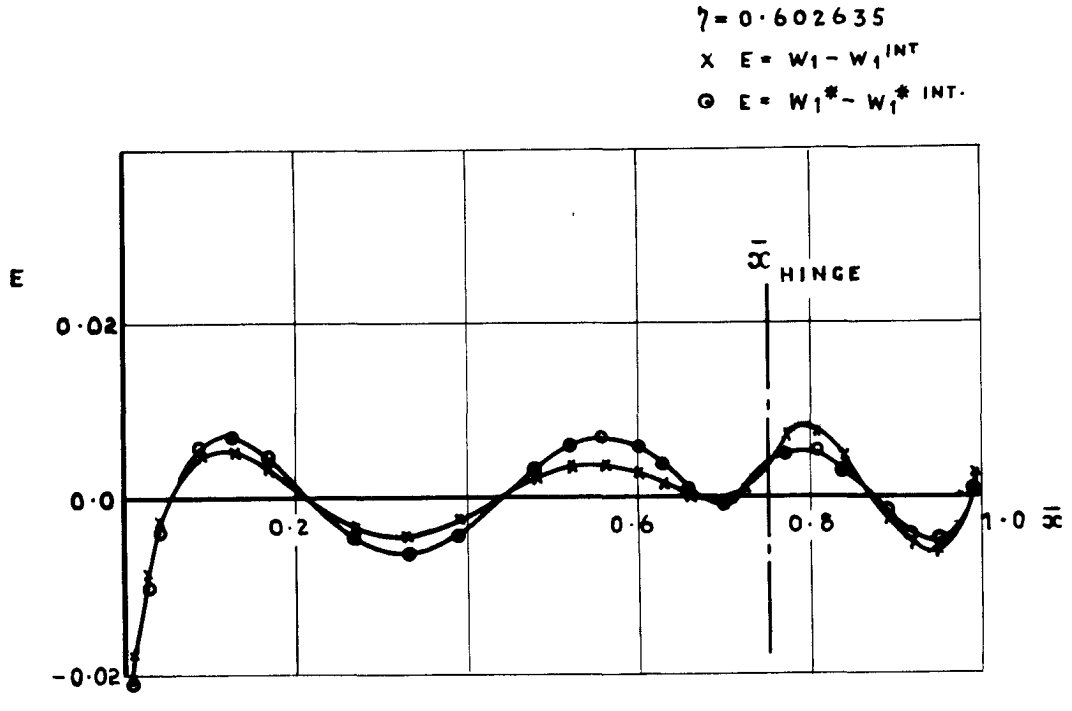

ERROR FUNCTION VS $\bar{x}$ FOR CONSTANT η

$(m,n) = (16,6)$, $A = 4$, $\Lambda = 45°$, $M = 0$

CONTROL SURFACES LOCATED IN $0.5 < |\eta| < 1$

$\zeta_{HINGE} = 0$ $(\bar{x} = 0.75)$

$\eta = 0.982973$

× $E = W_1 - W_1^{INT}$

⊙ $E = W_1^* - W_1^{*INT}$

INT = INTERPOLATED

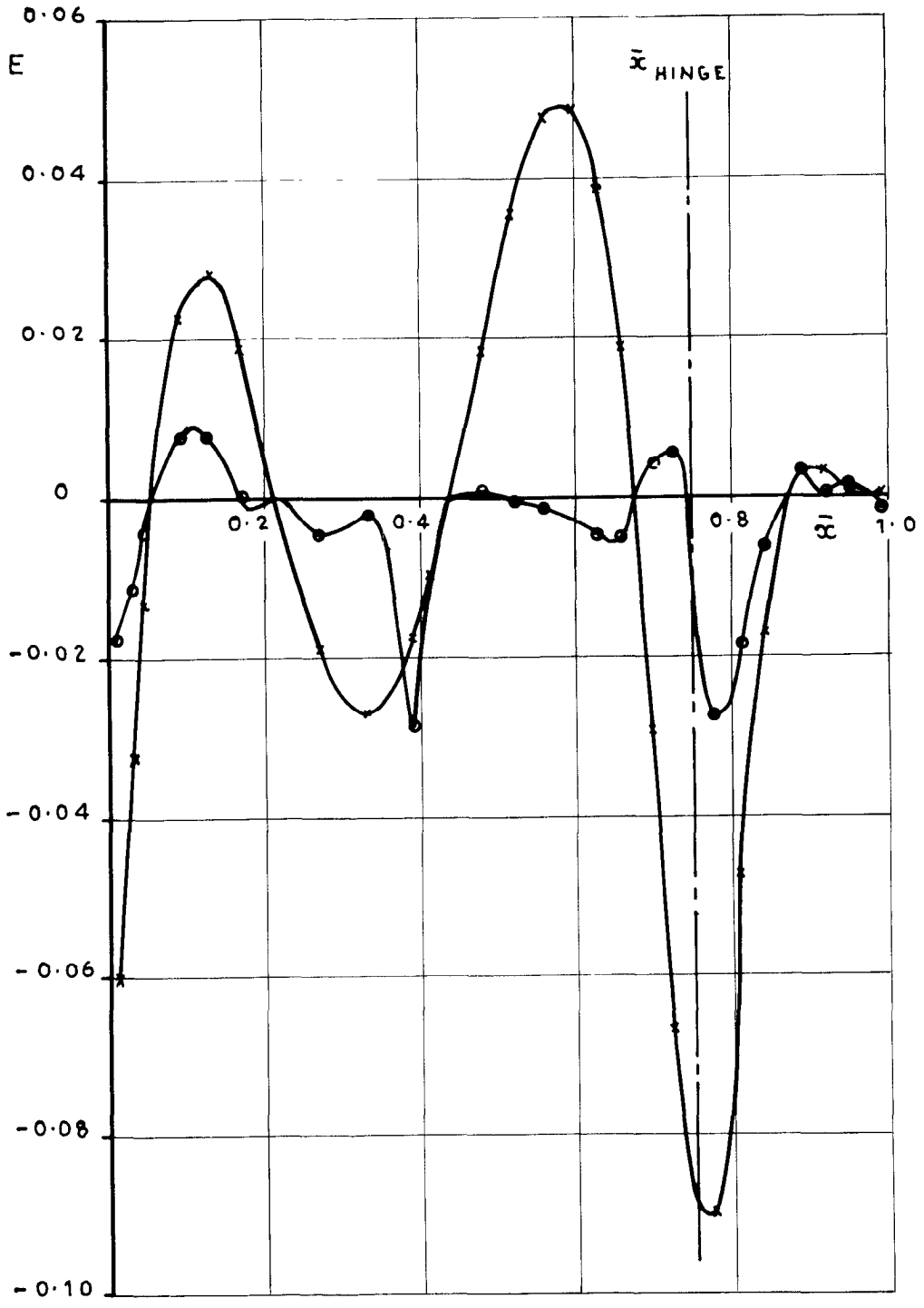

ΔC_p vs $\bar{x}$ FOR CONSTANT η, M=0·0 FOR A=4, Λ=45° WING WITH CONTROL SURFACES IN $0.5 < |\eta| < 1$ AND $\eta_{EDGE} = 0.5$.

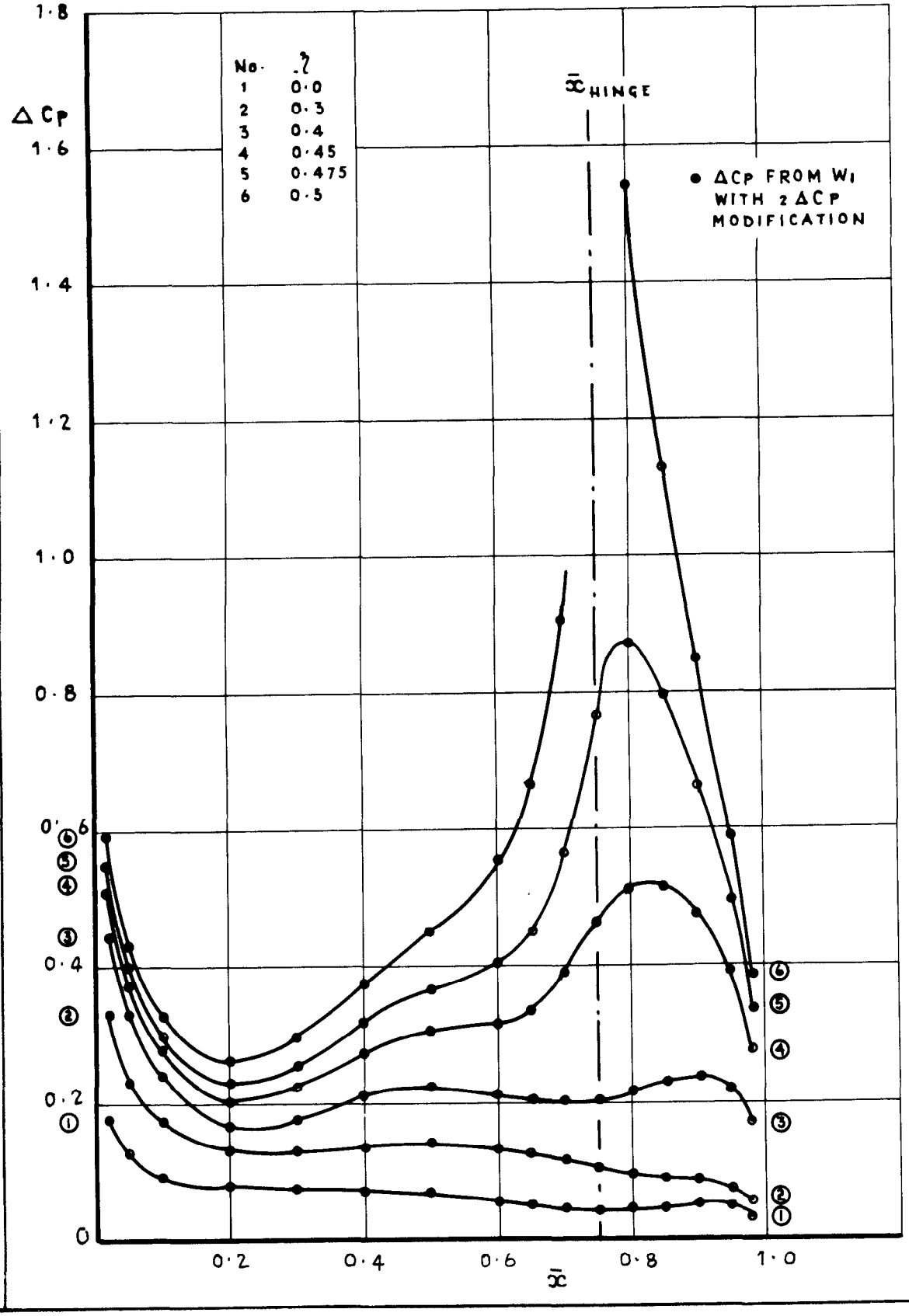

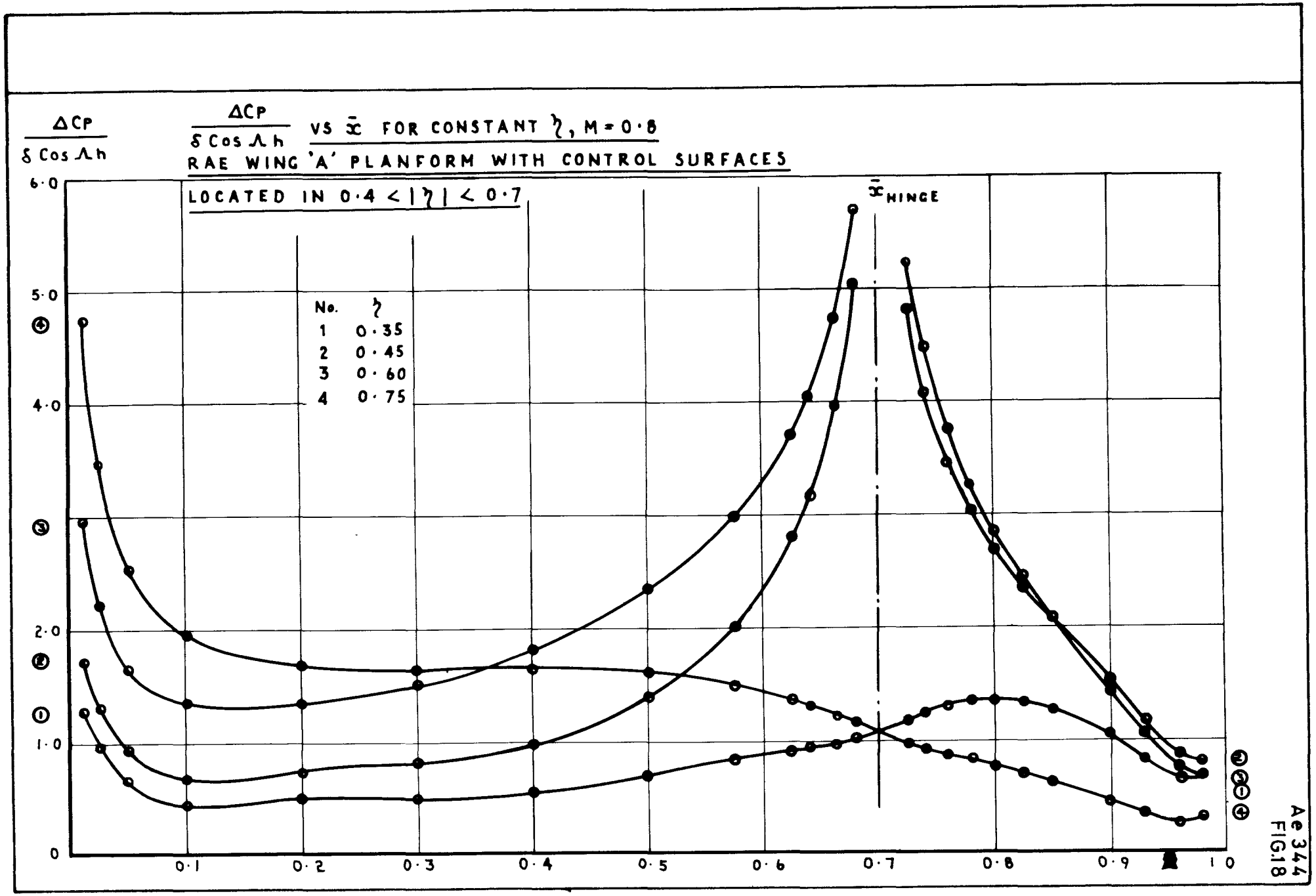
ΔCp / δ Cos Λh
ΔCp / δ Cos Λh VS x̄ FOR CONSTANT η, M = 0·8
RAE WING 'A' PLANFORM WITH CONTROL SURFACES
LOCATED IN 0·4 < |η| < 0·7
x̄ HINGE
No. η
1 0·35
2 0·45
3 0·60
4 0·75
6·0
5·0
4·0
2·0
1·0
0
0·1
0·2
0·3
0·4
0·5
0·6
0·7
0·8
0·9
1·0
Ae 344
FIG.18

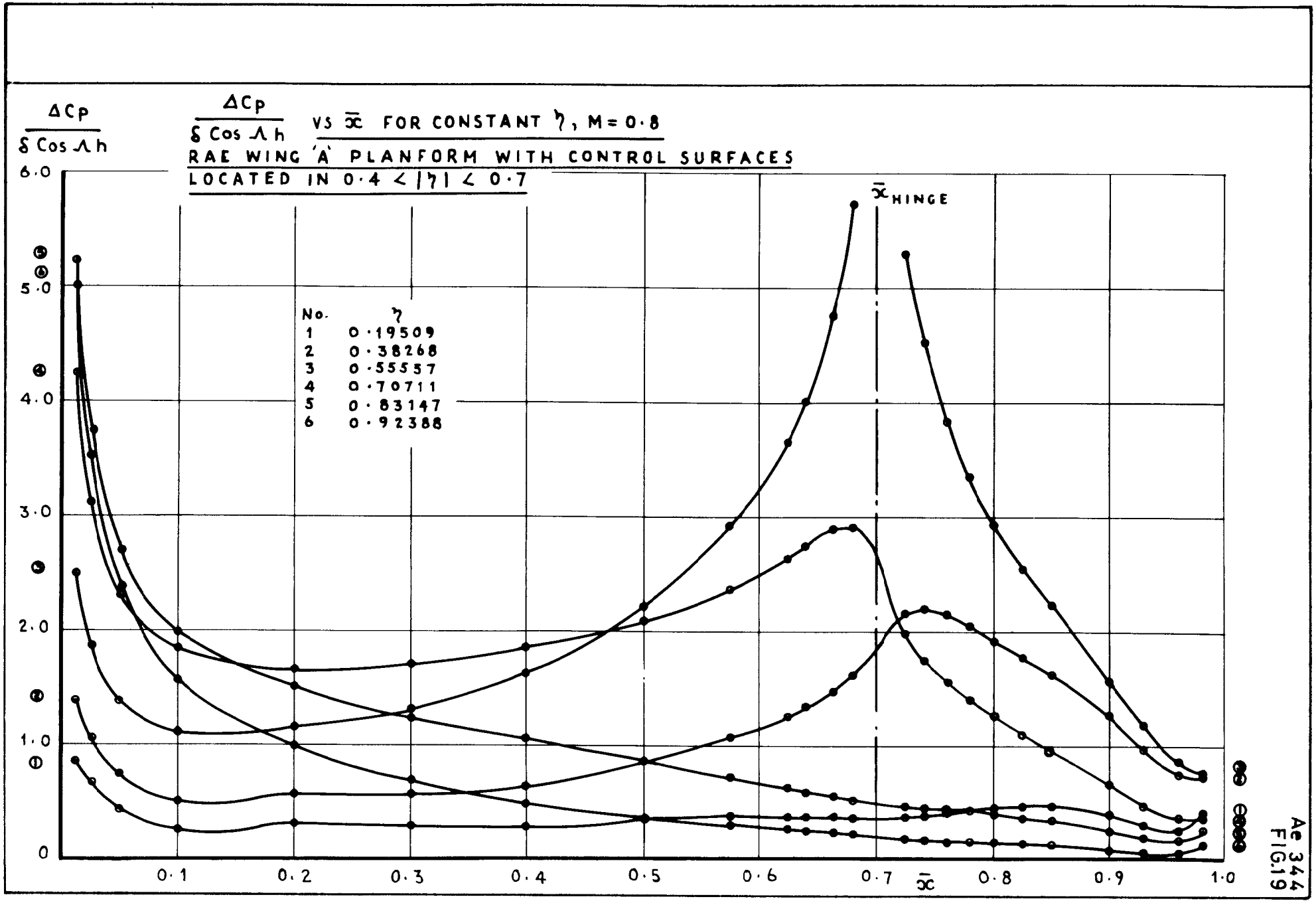
ΔCp / δ Cos Λh
ΔCp / δ Cos Λh VS x̄ FOR CONSTANT η, M = 0·8
RAE WING 'A' PLANFORM WITH CONTROL SURFACES
LOCATED IN 0·4 < |η| < 0·7
x̄ HINGE
No. η
1 0·19509
2 0·38268
3 0·55557
4 0·70711
5 0·83147
6 0·92388
6·0
5·0
4·0
3·0
2·0
1·0
0
0·1
0·2
0·3
0·4
0·5
0·6
0·7
x̄
0·8
0·9
1·0
Ae 344
FIG.19

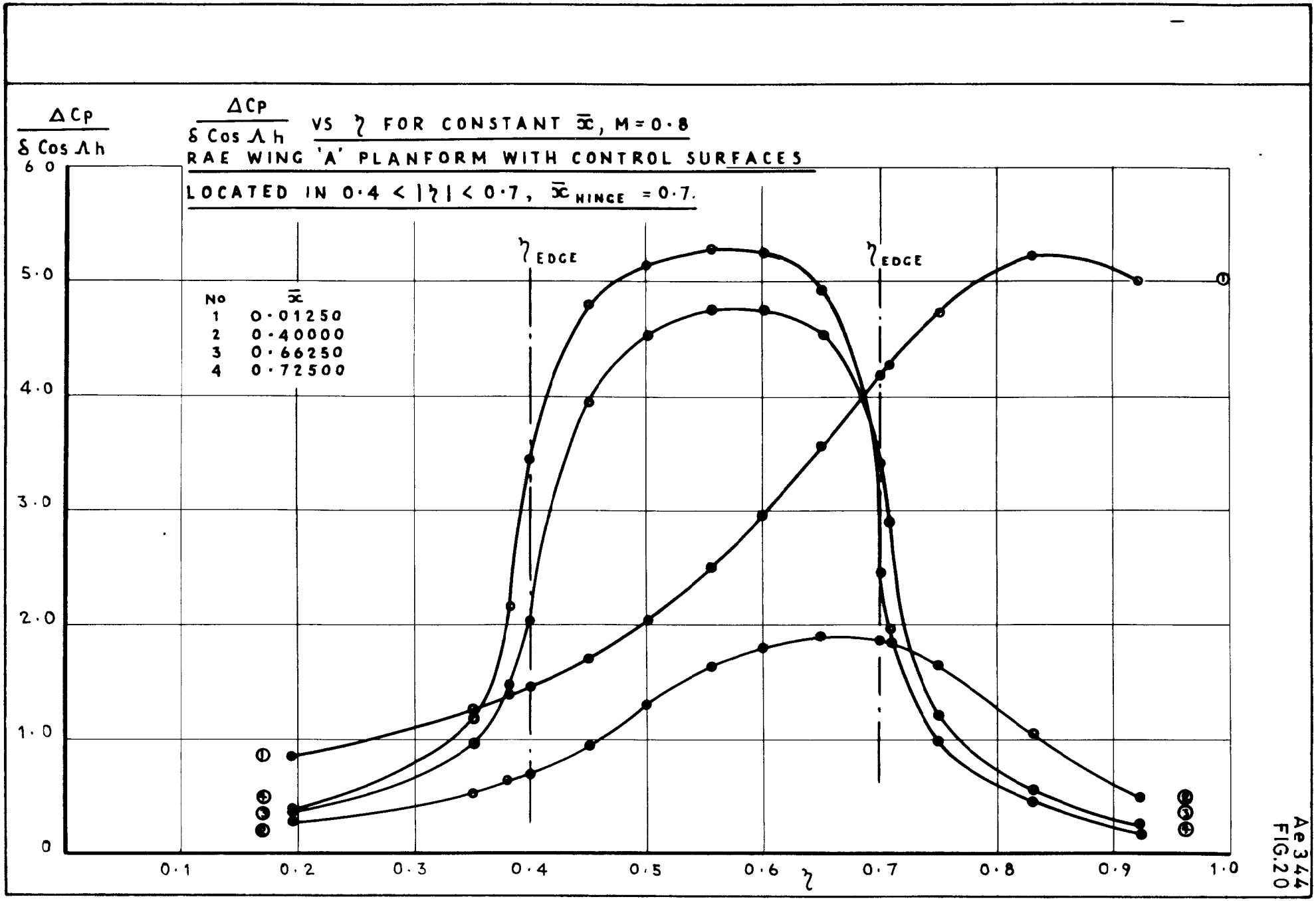
ΔCp / δ Cos Λh VS η FOR CONSTANT x̄, M = 0·8
RAE WING 'A' PLANFORM WITH CONTROL SURFACES
LOCATED IN 0·4 < |η| < 0·7, x̄ HINGE = 0·7.
No x̄
1 0·01250
2 0·40000
3 0·66250
4 0·72500
η EDGE
η EDGE
ΔCp / δ Cos Λh
6 0
5·0
4·0
3·0
2·0
1·0
0
0·1
0·2
0·3
0·4
0·5
0·6
0·7
0·8
0·9
1·0
η

Ae 344
FIG. 20

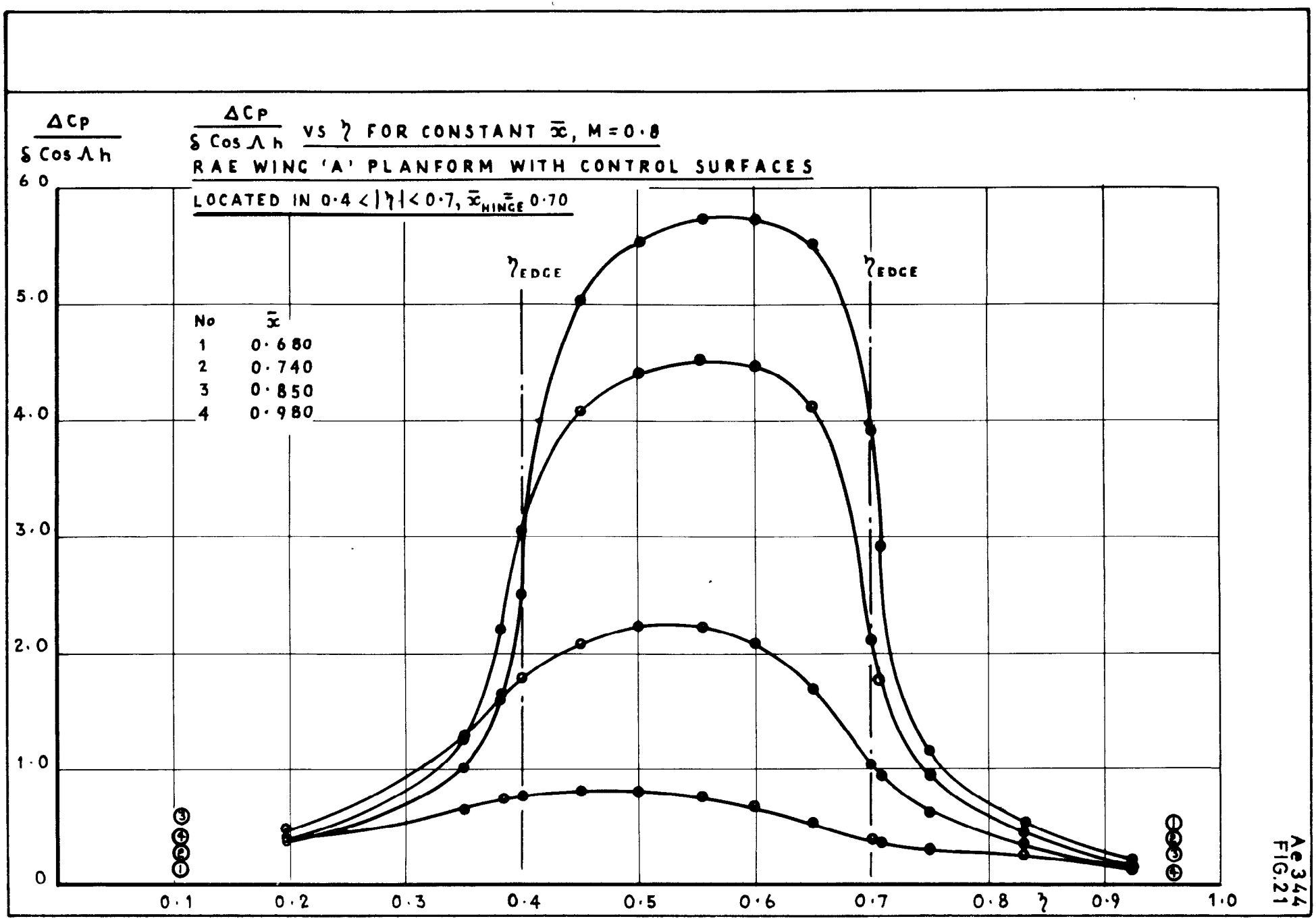
ΔCp / δ Cos Λh
ΔCp / δ Cos Λh VS η FOR CONSTANT x̄, M = 0·8
RAE WING 'A' PLANFORM WITH CONTROL SURFACES
LOCATED IN 0·4 < |η| < 0·7, x̄HINGE 0·70
No x̄
1 0·680
2 0·740
3 0·850
4 0·980
ηEDGE
ηEDGE
6·0
5·0
4·0
3·0
2·0
1·0
0
0·1
0·2
0·3
0·4
0·5
0·6
0·7
0·8
η
0·9
1·0

Ae 344
FIG. 21

Ae 344
FIG. 22

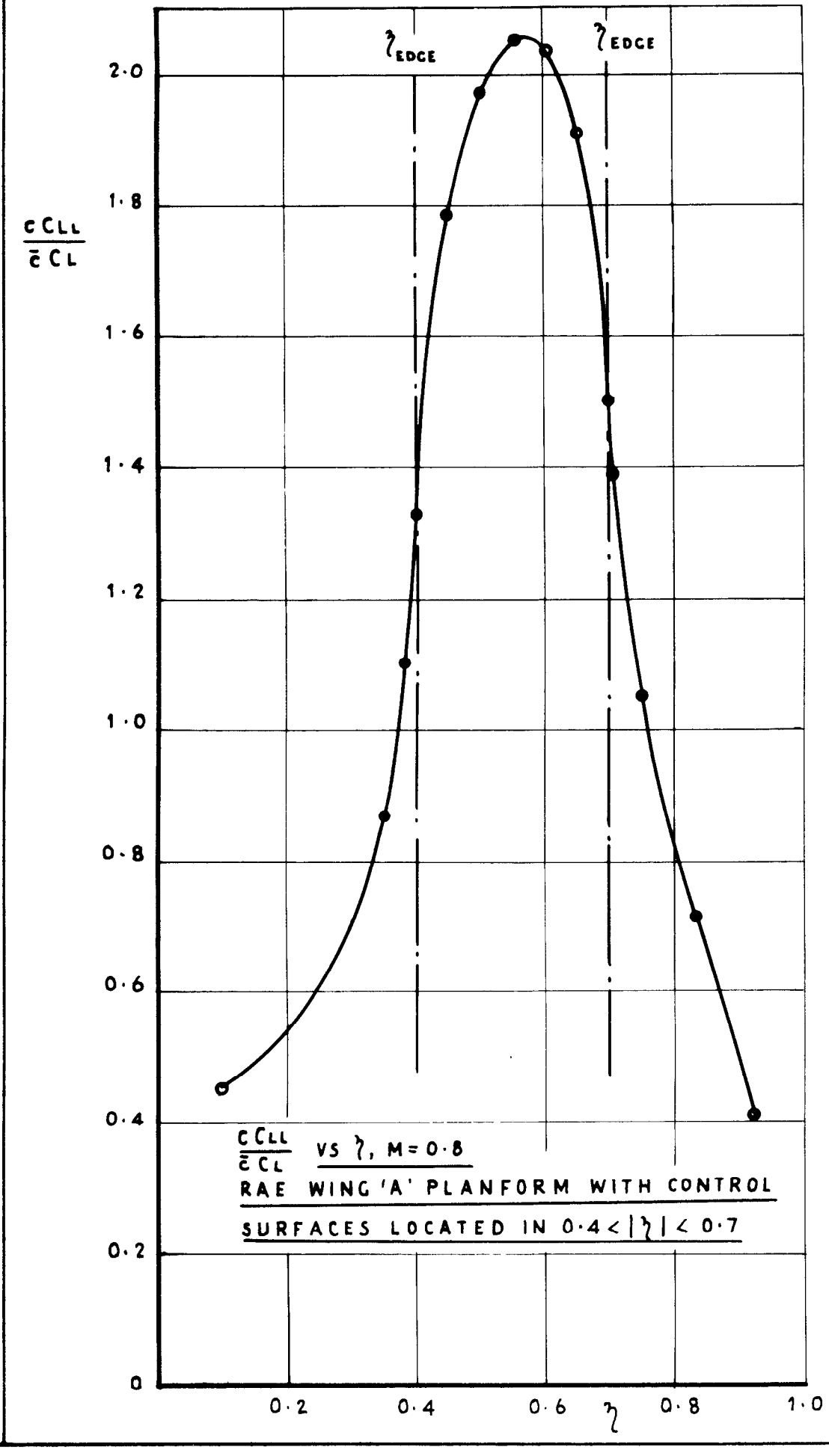

$\frac{c C_{LL}}{\bar{c} C_L}$ VS η, M = 0·8

RAE WING 'A' PLANFORM WITH CONTROL SURFACES LOCATED IN $0{\cdot}4 < |\eta| < 0{\cdot}7$

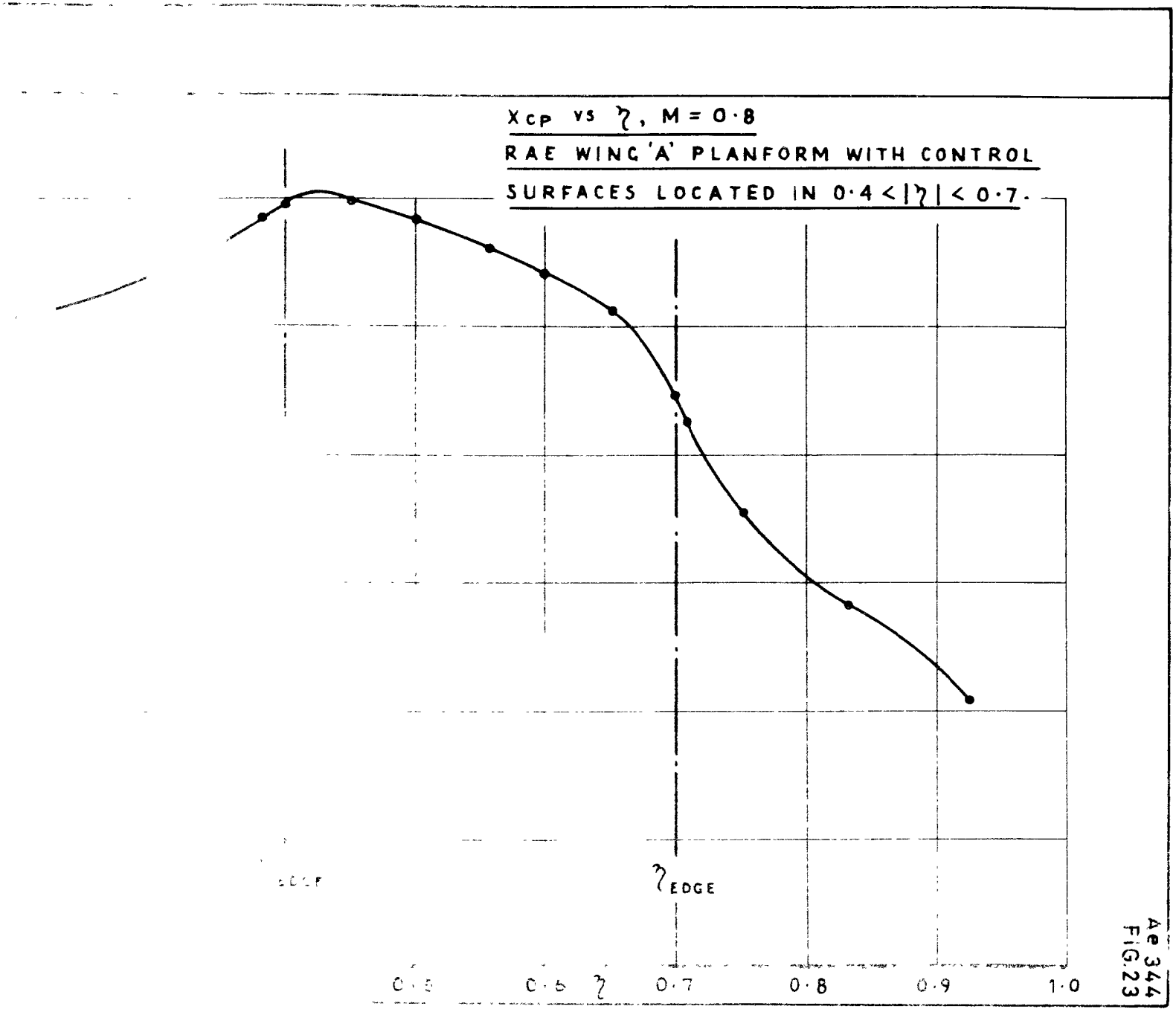
X_{CP} vs η, M = 0·8
RAE WING 'A' PLANFORM WITH CONTROL SURFACES LOCATED IN 0·4 < |η| < 0·7.
η_{EDGE}
0·5
0·6
η
0·7
0·8
0·9
1·0

Ae 344
FIG.23

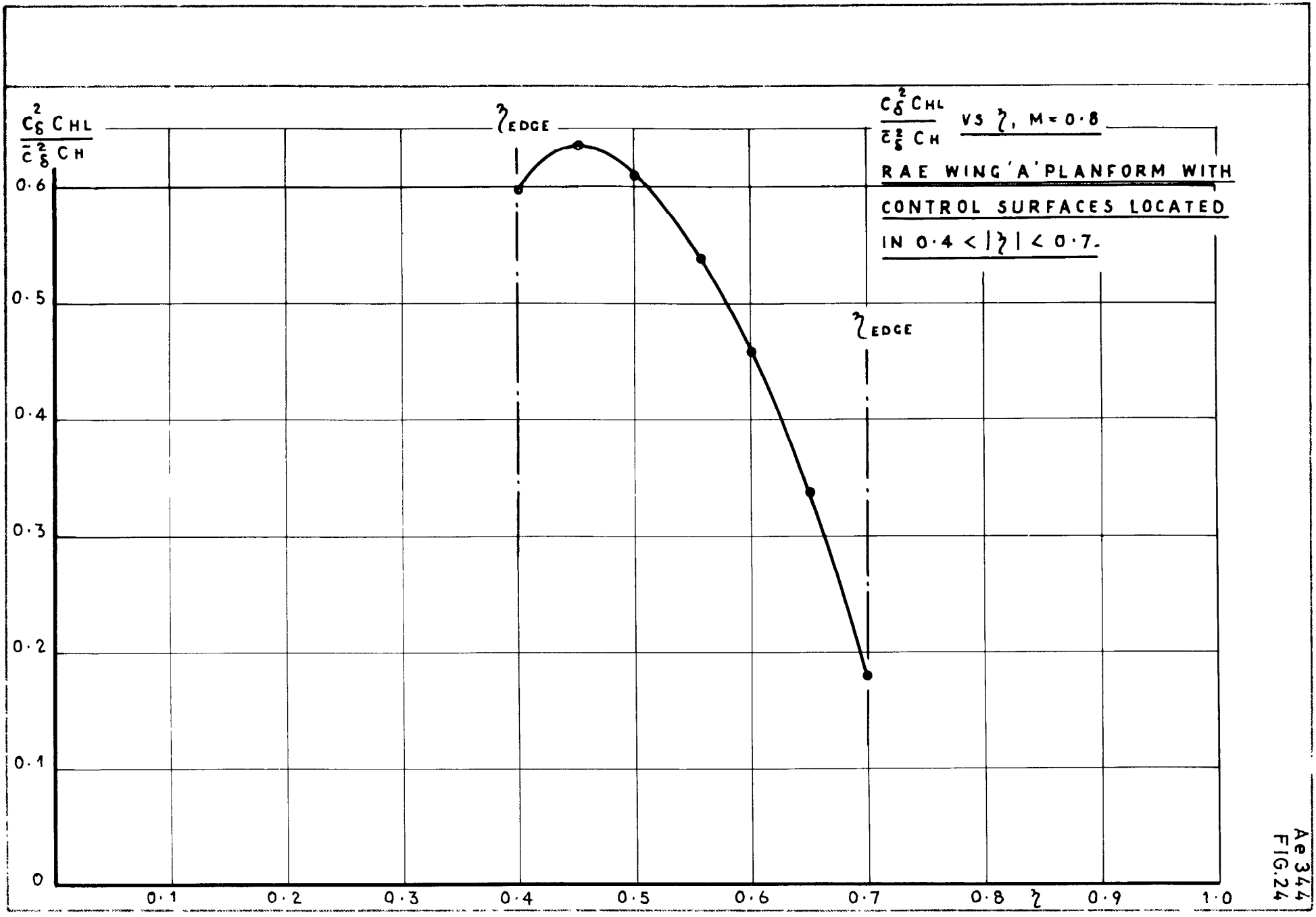
$\frac{C_\delta^2 C_{HL}}{\bar{c}_\delta^2 C_H}$
$\frac{C_\delta^2 C_{HL}}{\bar{c}_\delta^2 C_H}$ VS η, M = 0·8
RAE WING 'A' PLANFORM WITH CONTROL SURFACES LOCATED IN 0·4 < |η| < 0·7.
η_{EDGE}
η_{EDGE}
0·6
0·5
0·4
0·3
0·2
0·1
0
0·1
0·2
0·3
0·4
0·5
0·6
0·7
0·8
η
0·9
1·0

Ae 344
FIG. 24

ARC CP No.1340
January 1975
Wigley, T.G.

EVALUATION OF A LOADING FORM FOR THE CALCULATION OF LINEARISED THEORY PRESSURE DISTRIBUTIONS IN WINGS WITH CONTROL SURFACES HAVING SWEPT HINGE LINES IN STEADY SUBSONIC FLOW

Following suggestions made in BAC Preston Div. Rep. Ae311 (BR 24598) 'partıally matched' loadings are constructed to enable the accurate simulatıon of first order boundary conditions on wings with control surfaces having swept hinge lines ın subsonic flow. These loadings are assessed by observing the character of the difference between the induced downwash and the required boundary/

ARC CP No.1340
January 1975
Wigley, T.G.

EVALUATION OF A LOADING FORM FOR THE CALCULATION OF LINEARISED THEORY PRESSURE DISTRIBUTIONS IN WINGS WITH CONTROL SURFACES HAVING SWEPT HINGE LINES IN STEADY SUBSONIC FLOW

Following suggestions made in BAC Preston Div. Rep. Ae311 (BR 24598) 'partially matched' loadings are constructed to enable the accurate simulatıon of first order boundary conditions on wings with control surfaces having swept hinge lines in subsonic flow. These loadings are assessed by observing the character of the difference between the induced downwash and the required boundary/

ARC CP No.1340
January 1975
Wigley, T.G.

EVALUATION OF A LOADING FORM FOR THE CALCULATION OF LINEARISED THEORY PRESSURE DISTRIBUTIONS IN WINGS WITH CONTROL SURFACES HAVING SWEPT HINGE LINES IN STEADY SUBSONIC FLOW

Following suggestions made in BAC Preston Div. Rep. Ae311 (BR 24598) 'partially matched' loadings are constructed to enable the accurate simulation of first order boundary conditions on wings with control surfaces having swept hinge lines in subsonic flow. These loadings are assessed by observing the character of the difference between the induced downwash and the required boundary/

ARC CP No.1340
January 1975
Wigley, T.G.

EVALUATION OF A LOADING FORM FOR THE CALCULATION OF LINEARISED THEORY PRESSURE DISTRIBUTIONS IN WINGS WITH CONTROL SURFACES HAVING SWEPT HINGE LINES IN STEADY SUBSONIC FLOW

Following suggestions made in BAC Preston Div. Rep. Ae311 (BR 24598) 'partially matched' loadings are constructed to enable the accurate simulation of first order boundary conditions on wings with control surfaces having swept hinge lines in subsonic flow. These loadings are assessed by observing the character of the difference between the induced downwash and the required boundary/

boundary condition, paying special attention to the neighbourhoods of hinge line corners. Finally, the 'regularised' downwashes are used in lifting surface calculations to provide values for the 'fully matched' loadings.

boundary condition, paying special attention to the neighbourhoods of hinge line corners. Finally, the 'regularised' downwashes are used in lifting surface calculations to provide values for the 'fully matched' loadings.

boundary condition, paying special attention to the neighbourhoods of hinge line corners. Finally, the 'regularised' downwashes are used in lifting surface calculations to provide values for the 'fully matched' loadings.

boundary condition, paying special attention to the neighbourhoods of hinge line corners. Finally, the 'regularised' downwashes are used in lifting surface calculations to provide values for the 'fully matched' loadings.

HER MAJESTY'S STATIONERY OFFICE

Government Bookshops

49 High Holborn, London WC1V 6HB
13a Castle Street, Edinburgh EH2 3AR
41 The Hayes, Cardiff CF1 1JW
Brazennose Street, Manchester M60 8AS
Southey House, Wine Street, Bristol BS1 2BQ
258 Broad Street, Birmingham B1 2HE
80 Chichester Street, Belfast BT1 4JY

Government publications are also available through booksellers

C.P. No. 1340

ISBN 0 11 470950 5